



# Phenyl 4-(2-oxopyrrolidin-1-yl)benzenesulfonates and phenyl 4-(2-oxopyrrolidin-1-yl)benzenesulfonamides as new antimicrotubule agents targeting the colchicine-binding site

Mathieu Gagné-Boulet <sup>a, b</sup>, Chahrazed Bouzriba <sup>a, b</sup>, Atziri Corin Chavez Alvarez <sup>a, b</sup>, Sébastien Fortin <sup>a, b, \*</sup>

<sup>a</sup> Centre de recherche du CHU de Québec - Université Laval, Axe oncologie, Hôpital Saint-François d'Assise, 10 rue de l'Espinay, Québec, QC, G1L 3L5, Canada

<sup>b</sup> Faculté de pharmacie, Université Laval, Québec, QC, G1V 0A6, Canada



## ARTICLE INFO

### Article history:

Received 13 October 2020  
Received in revised form  
23 December 2020  
Accepted 24 December 2020  
Available online 6 January 2021

### Keywords:

Anticancer agents  
Antimicrotubule agents  
Antimitotics  
Colchicine-binding site inhibitors  
Phenyl 4-(2-oxopyrrolidin-1-yl)  
benzenesulfonates  
Phenyl 4-(2-oxopyrrolidin-1-yl)  
benzenesulfonamides

## ABSTRACT

We recently designed and prepared new families of potent antimicrotubule agents designated as *N*-phenyl 4-(2-oxoimidazolidin-1-yl)benzenesulfonates (PIB-SOs) and phenyl 4-(2-oxoimidazolidin-1-yl)benzenesulfonamides (PIB-SAs). Our previous structure-activity relationship studies (SAR) focused on the aromatic ring B of PIB-SOs and PIB-SAs leaving the impact of the phenylimidazolidin-2-one moiety (ring A) on the binding to the colchicine-binding site (C-BS) poorly studied. Therefore, the aim of the present study was to evaluate the effect of replacing the imidazolidin-2-one (IMZ) group by a pyrrolidin-2-one moiety. To that end, 15 new phenyl 4-(2-oxopyrrolidin-1-yl)benzenesulfonate (PYB-SO) and 15 phenyl 4-(2-oxopyrrolidin-1-yl)benzenesulfonamide (PYB-SA) derivatives were designed, prepared, chemically characterised and biologically evaluated. PYB-SOs and PYB-SAs exhibit antiproliferative activity in the low nanomolar to low micromolar range (0.0087–8.6  $\mu$ M and 0.056–21  $\mu$ M, respectively) on human HT-1080, HT-29, M21 and MCF7 cancer cell lines. Moreover, they block cell cycle progression in G2/M phase. Immunofluorescence, tubulin affinity and tubulin polymerisation assays show that they cause microtubule depolymerisation by docking the C-BS. In addition, docking assays with the most potent derivatives show binding affinity toward the C-BS and they also exhibit weak or no toxicity toward chick embryos. Finally, physicochemical properties calculated using the SwissADME algorithm show that PYB-SOs and PYB-SAs are promising new families of antimicrotubule agents.

© 2020 Elsevier Masson SAS. All rights reserved.

## 1. Introduction

Cancer is a large class of diseases characterised by an uncontrolled and abnormal cellular growth causing serious health issues and ultimately leading to death if untreated. To this day, it is still one of the most important health problems in the world [1]. Indeed, cancer was responsible for approximately 9.6 million deaths worldwide in 2018 [2]. Despite major progress achieved in the past decades, many cancers are still having poor prognoses and high mortality rates [3]. In addition, some anticancer agents currently

used in clinical trials still have significant deleterious effects, limited effectiveness and are prone to induce chemoresistance. In this context, the development of new antimitotic drugs that aim to improve both the life expectancy and the quality of life of cancer patients is of uttermost importance [4].

Microtubules are the main constituents of the cytoskeleton in eukaryotic cells. They are composed of  $\alpha$ ,  $\beta$ -tubulin heterodimers which are in constant dynamic equilibrium between their polymerisation and depolymerisation states [5]. They participate in diverse cellular functions such as cell replication, maintenance of cell shape, mitosis, motility and cellular transport [6]. Therefore, microtubules are an important target in cancer chemotherapy. Antimicrotubule agents are divided into two main classes based on their effect on microtubules: microtubule-stabilising agents and microtubule-destabilising agents. Microtubule-stabilising agents bind to microtubules and stabilise the polymer while microtubule-destabilising agents bind to the tubulin heterodimers and

*Abbreviations:* Combretastatin A-4, CA-4; *N*-phenyl 4-(2-oxoimidazolidin-1-yl)benzenesulfonate, PIB-SOs; phenyl 4-(2-oxopyrrolidin-1-yl)benzenesulfonates, PYB-SOs; phenyl 4-(2-oxopyrrolidin-1-yl)benzenesulfonamides, PYB-SAs.

\* Corresponding author. Faculté de pharmacie, Université Laval, Québec, QC, G1V 0A6, Canada.

E-mail address: [sebastien.fortin@pha.ulaval.ca](mailto:sebastien.fortin@pha.ulaval.ca) (S. Fortin).

destabilise microtubules. Antimicrotubule agents such as paclitaxel (**1**, Fig. 1A) have been part of the armamentarium of physicians for treating cancer patients since the 1990s [7,8]. New antimicrotubule agents are still of interest for several reasons, notably to reduce their toxicity, to improve their effectiveness, to improve their selectivity for given tumours and to reduce their production costs. To that end, new antimicrotubule agents are in preclinical development and are currently undergoing clinical trials [9–11]. Some well-known previously studied compounds include combretastatin A-4 disodium phosphate (CA-4DP, **2**, Fig. 1B) [12] and T138067 sodium (**3**, Fig. 1C) [13].

To circumvent these impediments, our research group previously designed and developed two new families of antimicrotubule agents designated as phenyl 4-(2-oxoimidazolidin-1-yl)-benzenesulfonates (PIB-SOs, Fig. 1D) [14] and phenyl 4-(2-oxoimidazolidin-1-yl)-benzenesulfonamides (PIB-SAs, Fig. 1E) [15]. The molecular structures of PIB-SOs and PIB-SAs comprise two aromatic rings (A and B) linked either by a sulfonate or a sulfonamide bridge. The aromatic ring A is substituted by an imidazolidin-2-one (IMZ) moiety at position 4 while the aromatic ring B bears either a methoxyl group, short alkyl chain or halogen groups in position 3, 4 and/or 5. PIB-SO and PIB-SA derivatives exhibit antiproliferative activity in the nanomolar to low micromolar range on numerous human cancer cell lines, notably HT-1080 fibrosarcoma, HT-29 colon adenocarcinoma, M21 skin melanoma and MCF7 oestrogen-dependent breast adenocarcinoma. Moreover, they induce arrest of the cell cycle progression in G2/M phase and they cause microtubule depolymerisation and cytoskeleton disruption by targeting the colchicine-binding site (C-BS) located at the interface of the  $\alpha$ ,  $\beta$ -tubulin heterodimer [14,15].

Previous structure-activity relationship (SAR) studies were focusing almost exclusively on the aromatic ring B and showed that the substitution in positions 3, 3,5 or 3,4,5 is required to maintain both the antiproliferative activity in the nanomolar range and the

high-binding affinity for the C-BS. SAR studies on the aromatic ring A evidenced that the IMZ moiety cannot be modified easily without losing the biological activity [14–17]. In addition, our molecular modeling experiments using PIB-SOs and PIB-SAs suggested that the substituent shape is more important than hydrogen bonds and electrostatic forces since the binding pocket is clearly hydrophobic and mostly driven by van der Waals forces [16]. Consequently, the importance of the NH group of the IMZ moiety for the interaction of PIB-SOs and PIB-SAs with the C-BS remains to be studied.

In this study, we investigate the impact of the NH group of the IMZ moiety of PIB-SOs and PIB-SAs on the biological activity by replacing the NH group by a CH<sub>2</sub> group. Therefore, a new series of phenyl 4-(2-oxopyrrolidin-1-yl)benzenesulfonates (PYB-SOs, Fig. 1E) as well as a new series of 4-(2-oxopyrrolidin-1-yl)-*N*-phenylbenzenesulfonamides (PYB-SAs, Fig. 1F) were prepared. PYB-SOs and PYB-SAs were first assessed for their antiproliferative activity on HT-1080, HT-29, M21 and MCF7 human cancer cell lines. The most potent compounds were assessed for their potential to arrest M21 cell cycle progression. Afterwards, they were evaluated for their potency to disrupt the cytoskeleton and inhibit microtubule polymerisation. Furthermore, we assessed our most potent derivatives for their binding affinity for the C-BS and their toxicity on chick embryos. Finally, their biopharmaceutical properties were assessed using SwissADME free web tool [18].

## 2. Chemistry

The preparation of PYB-SOs (**4–18**) and PYB-SAs (**19–33**) is depicted in Scheme 1 and was achieved within 4 steps. Briefly, the general synthesis started with the nucleophilic addition of aniline on 4-chlorobutanoyl chloride in presence of triethylamine in methylene chloride followed by the intramolecular cyclization of 4-chloro-*N*-phenylbutanamide (**34**) into 1-phenylpyrrolidin-2-one (**35**) by addition of sodium hydride in tetrahydrofuran.

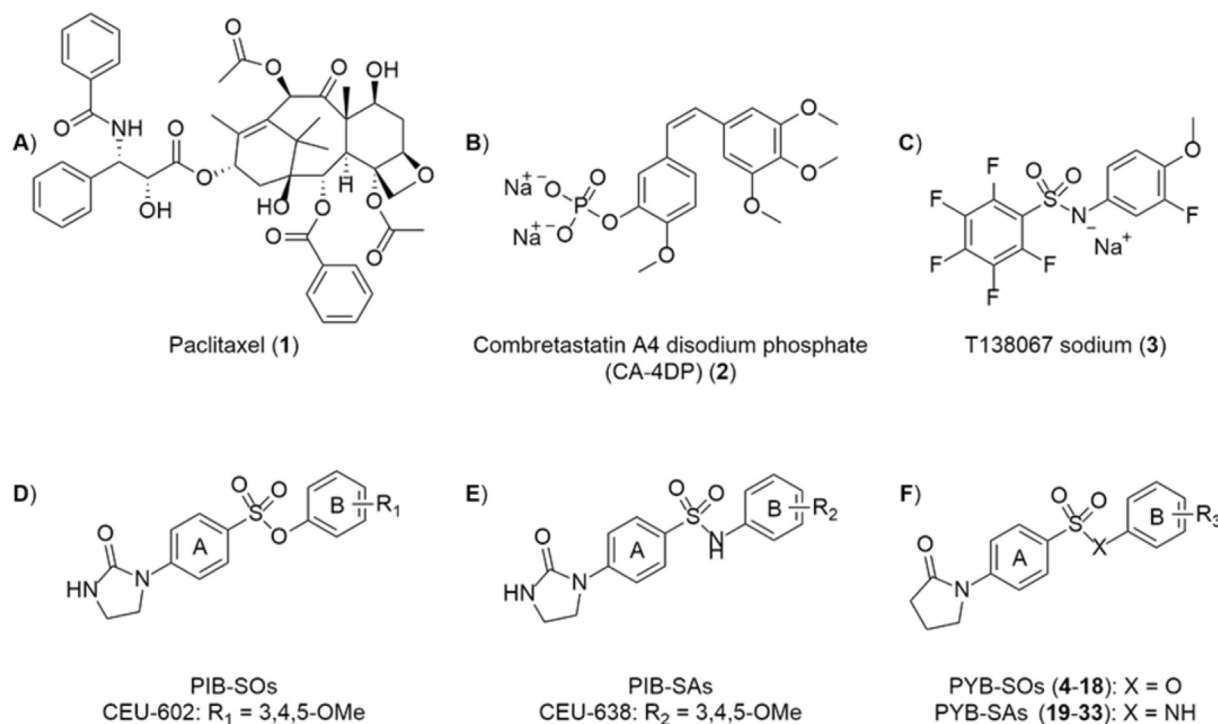
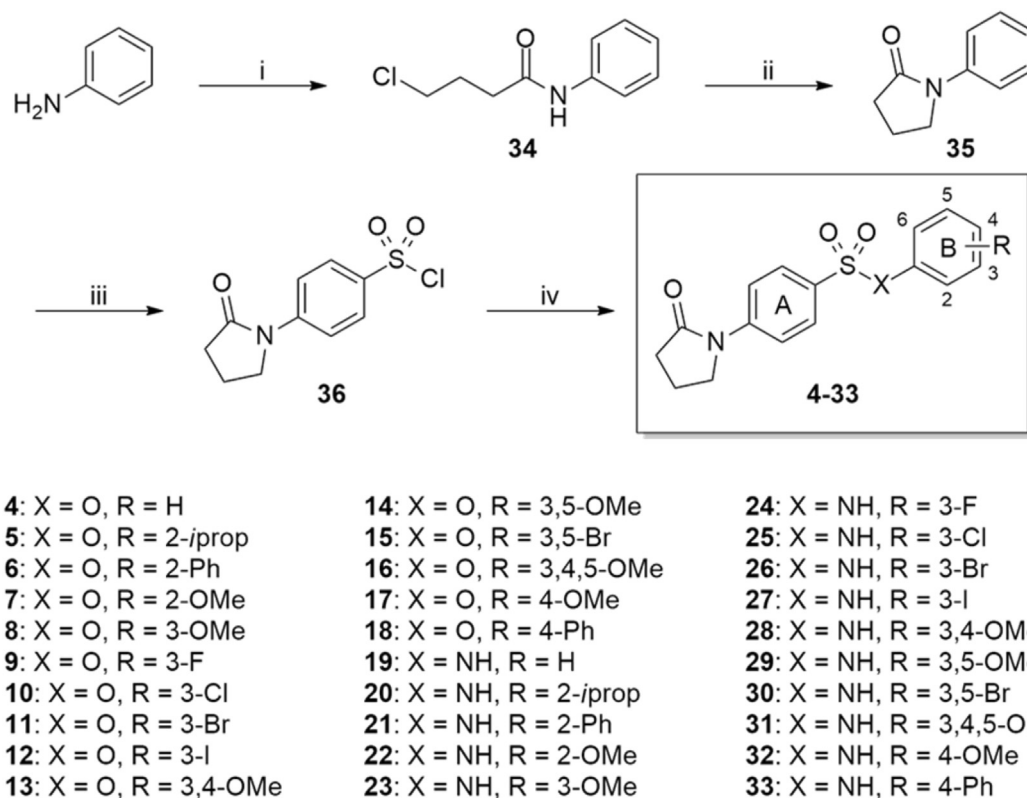


**Fig. 1.** Molecular structures of antimicrotubule agents A) paclitaxel (**1**), B) combretastatin A-4 disodium phosphate (CA-4DP, **2**), C) T138067 sodium (**3**), D) *N*-phenyl 4-(2-oxoimidazolidin-1-yl)benzenesulfonates (PIB-SOs), E) phenyl 4-(2-oxoimidazolidin-1-yl)benzenesulfonamides (PIB-SAs) F) phenyl 4-(2-oxopyrrolidin-1-yl)benzenesulfonates (PYB-SOs, **4–18**) and phenyl 4-(2-oxopyrrolidin-1-yl)-*N*-phenylbenzenesulfonamides (PYB-SAs, **19–33**).



**Scheme 1.** Reagents and conditions: (i) 4-chlorobutanoyl chloride,  $\text{CH}_2\text{Cl}_2$ , rt, 24 h, 78%; (ii) NaH, THF, 0 °C to rt, 24 h, 86%; (iii)  $\text{ClSO}_3\text{H}$ , 0 °C to rt, overnight, 72%; (iv) relevant phenol, TEA,  $\text{CH}_3\text{CN}$ , 120 °C under microwaves, 8 h, 31–97% or relevant aniline, DMAP,  $\text{CH}_3\text{CN}$ , 120 °C under microwaves, 8 h, 18–67%.

Chlorosulfonation of **35** with chlorosulfonic acid gave the 4-(2-oxopyrrolidin-1-yl)benzenesulfonyl chloride (**36**). Finally, PYB-SOs (**4–18**) and PYB-SAs (**19–33**) were prepared by the nucleophilic addition of a relevant phenol in presence of triethylamine or a relevant aniline in presence of 4-dimethylaminopyridine to **36** in acetonitrile under microwaves.

### 3. Results/discussion

#### 3.1. PYB-SOs and PYB-SAs exhibit antiproliferative activity on human cancer cells

The antiproliferative activity of PYB-SOs (**4–18**) and PYB-SAs (**19–33**) was assessed on the HT-1080 fibrosarcoma, HT-29 colon adenocarcinoma, M21 skin melanoma and MCF7 oestrogen-dependent breast adenocarcinoma using the sulforhodamine B colorimetric assay and the results are listed in Table 1 and correspond to the concentration of drug needed to inhibit 50% of cell growth ( $\text{IC}_{50}$ ). Combretastatin A-4 (CA-4), PIB-SO (CEU-602) and PIB-SA (CEU-634) bearing a 3,4,5 trimethoxyl group on ring B that were the most potent PIB-SO and PIB-SA prepared so far were used as positive controls [14,15]. PYB-SOs and PYB-SAs exhibit antiproliferative activity ranging from the low nanomolar to the low micromolar levels on all cancer cell lines tested (0.0087–8.6  $\mu\text{M}$  for PYB-SOs and 0.056–21  $\mu\text{M}$  for PYB-SAs, respectively). Globally, PYB-SOs are more potent than their PYB-SA counterparts. The sensitivity of cell lines to PYB-SOs and PYB-SAs usually decreases according to the following order: MCF7 > HT-29  $\approx$  M21 > HT-1080. The disubstitution of the aromatic ring B in positions 3 and 5 by methoxyl and bromo groups and trisubstitution in positions 3, 4 and 5 by methoxyl groups are the most favourable substitutions leading to maximal antiproliferative activities. PYB-SOs **15** and

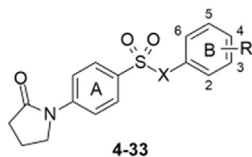
PYB-SAs **31** are the most potent derivatives with  $\text{IC}_{50}$  ranging from 8.7 to 11 nM and 56–130 nM, respectively. Furthermore, the most active PYB-SOs, bearing either a 3,5-dimethoxyl (**14**), a 3,5-dibromo (**15**) or a 3,4,5-trimethoxyl (**16**) groups exhibited antiproliferative activities (8.7–39 nM) similar to CA-4 (1.9–5.1 nM), CEU-602 (4.0–5.9 nM) and CEU-638 (13–21 nM) used as positive controls. Finally, these results confirm that the NH group of IMZ moiety of PIB-SOs is not essential to the antiproliferative activity.

#### 3.2. PYB-SO and PYB-SA derivatives arrest the cell cycle progression in G2/M phase

Antimicrotubule agents are known to arrest cell cycle progression during the G2/M phase. To verify the mechanism of action underlying the antiproliferative activity of PYB-SOs and PYB-SAs with PIB-SOs and PIB-SAs that were used as molecular scaffolds, we first assessed their effect on the cell cycle progression of M21 cells [14,15]. To that end, PYB-SOs **11**, **12** and **14–16**, and PYB-SAs **21**, **25**, **27** and **29–31** were incubated with M21 cells at 2 and 5-times their respective  $\text{IC}_{50}$  for 24 h. The results depicted in Fig. 2 show the optimal concentration (either 2 or 5-times the  $\text{IC}_{50}$ ) for a maximal arrest of cell cycle progression in the G2/M phase. As shown in Fig. 2, cells treated with 0.5% DMSO (negative control) were at 5.0, 65.5, 16.1 and 13.4% in subG1, G0/G1, S and G2/M phases, respectively. CA-4 was used as positive control and showed a population increase in G2/M phase by 66.1%. Except PYB-SA **21** bearing a phenyl substituent in position 2, all PYB-SOs and PYB-SAs assessed increased the cell population in G2/M phase by 28.8–68.4%. Furthermore, PYB-SOs and PYB-SAs bearing the same substituent have a similar effect on the cell cycle progression which indicates that the modification of the sulfonate bridge by a sulfonamide moiety does not affect their ability to arrest the cell cycle

**Table 1**

Antiproliferative activity (IC<sub>50</sub>) of PYB-SOs (**4–18**) and PYB-SAs (**19–33**) on HT-1080, HT-29, M21 and MCF7 human cancer cell lines.



#	X	R	IC <sub>50</sub> (nM) <sup>a</sup>			
			HT-1080	HT-29	M21	MCF7
<b>4</b>	O	H	920	480	460	650
<b>5</b>	O	2- <i>i</i> prop	840	780	910	500
<b>6</b>	O	2-Ph	370	350	190	210
<b>7</b>	O	2-OMe	1300	1200	1300	890
<b>8</b>	O	3-OMe	190	120	120	100
<b>9</b>	O	3-F	810	310	300	370
<b>10</b>	O	3-Cl	180	120	110	140
<b>11</b>	O	3-Br	80	60	40	60
<b>12</b>	O	3-I	40	59	88	22
<b>13</b>	O	3,4-OMe	590	690	650	290
<b>14</b>	O	3,5-OMe	26	39	12	21
<b>15</b>	O	3,5-Br	11	10	8.7	11
<b>16</b>	O	3,4,5-OMe	11	16	13	17
<b>17</b>	O	4-OMe	8500	4800	7500	4600
<b>18</b>	O	4-Ph	2600	2900	2300	1700
<b>19</b>	NH	H	4900	3400	5600	2800
<b>20</b>	NH	2- <i>i</i> prop	21000	12000	9900	16000
<b>21</b>	NH	2-Ph	1200	730	430	960
<b>22</b>	NH	2-OMe	3200	2400	3000	1800
<b>23</b>	NH	3-OMe	1300	860	940	1100
<b>24</b>	NH	3-F	840	5400	2300	680
<b>25</b>	NH	3-Cl	680	680	770	560
<b>26</b>	NH	3-Br	1300	590	950	830
<b>27</b>	NH	3-I	860	390	330	600
<b>28</b>	NH	3,4-OMe	2250	890	5100	2600
<b>29</b>	NH	3,5-OMe	990	1300	390	690
<b>30</b>	NH	3,5-Br	590	390	280	520
<b>31</b>	NH	3,4,5-OMe	130	80	56	88
<b>32</b>	NH	4-OMe	8500	4800	7500	4600
<b>33</b>	NH	4-Ph	8800	5400	4700	7000
<b>CEU-602</b>	O	3,4,5-OMe	5.9	4.0	4.0	5.0
<b>CEU-638</b>	NH	3,4,5-OMe	17	21	13	18
<b>CA-4<sup>b</sup></b>	N/A	N/A	2.2	5.1	2.2	1.9

<sup>a</sup> IC<sub>50</sub>: concentration of drug inhibiting cell growth by 50%.

<sup>b</sup> CA-4: Combretastatin A-4.

progression in the G<sub>2</sub>/M phase. In general, PYB-SOs and PYB-SAs bearing multiple substitutions have higher potential to arrest the cell cycle in G<sub>2</sub>/M phase than those bearing only one substitution. Finally, PYB-SO **16** exhibits the most potent cell cycle arrest in G<sub>2</sub>/M phase showing a population increase in G<sub>2</sub>/M phase by 68.4% which is similar to CA-4.

### 3.3. PYB-SOs and PYB-SAs induce cytoskeleton disruption

Since PYB-SOs and PYB-SAs arrest cell cycle progression in the G<sub>2</sub>/M phase, we evaluated their ability to induce cytoskeleton disruption by interfering with microtubules. To that end, we selected our 3 most potent PYB-SOs (**14–16**) and PYB-SAs (**27, 30** and **31**) for their effect on microtubules and cytoskeleton integrity of M21 cells when they are incubated at 5-times their respective IC<sub>50</sub> for 24 h. Cellular microtubule structures were visualised with indirect immunofluorescence using an anti-β-tubulin monoclonal antibody. CA-4 and paclitaxel were used as positive controls while DMSO (0.5%) was used as negative control. As depicted in Fig. 3, PYB-SOs and PYB-SAs disrupt microtubules and induce mitotic abnormalities similarly to CA-4. Therefore, PYB-SOs and PYB-SAs

are antimicrotubule agents inducing cytoskeleton disruption similarly as reported for CA-4, CEU-602 and CEU-638 [14,15].

### 3.4. PYB-SOs and PYB-SAs inhibit microtubule polymerisation

To confirm the effect of PYB-SOs and PYB-SAs on microtubules, we assessed the effect of PYB-SOs **14** and **15** and PYB-SAs **30** and **31** on dynamic polymerisation of tubulin to microtubules [19]. The curves shown in Fig. 4 are representative of 2 separated experiments. As shown in Fig. 4, microtubule formation rates are displayed over a period of 60 min at 37 °C. 15 μM of a microtubule-destabilising agent (CA-4) and 3 μM of a microtubule-stabilising agent (paclitaxel) were used as positive controls while DMSO (0.5%) was used as negative control. The concentrations of PYB-SOs **14** (30 μM) and **15** (3 μM) as well as PYB-SAs **30** (3 μM) and **31** (15 μM) were determined by maximal solubility in the buffer solution. Our results show that CA-4 inhibits tubulin polymerisation while paclitaxel stabilises it. PYB-SOs **14** and **15** and PYB-SAs **31** strongly inhibit tubulin polymerisation similarly to CA-4 while the inhibition of tubulin polymerisation by PYB-SA **30** is slightly lower. PYB-SA **31** show the most potent inhibition of tubulin polymerisation. These results strongly indicate that the mechanism of action of PYB-SOs and PYB-SAs is the inhibition of polymerisation of tubulin to microtubules.

### 3.5. PYB-SOs and PYB-SAs bind to the colchicine-binding site

It is known that antimicrotubule agents can interact with microtubules or tubulin heterodimers through different binding sites [20]. Moreover, PIB-SOs, PIB-SAs and CA-4 are known to dock into the C-BS [14,15]. In this context, we used a detection technique developed by our laboratory to study the binding of PYB-SOs and PYB-SAs with the C-BS [21]. This assay is based on the *N,N'*-ethylene-bis(iodoacetamide) (EBI) which crosslinks cysteines in positions 239 and 354 located in the C-BS. This adduct is conveniently detectable by Western blot as a second immunoreacting band of β-tubulin. Antimicrotubule compounds that bind to the C-BS inhibits the formation of the β-tubulin adduct with EBI. To that end, we also used PYB-SOs **14–16**, and PYB-SAs **27, 30**, and **31** at 100 and 1000-times their respective IC<sub>50</sub>. The maximum concentration used in this experiment was 100 μM. As displayed in Fig. 5, all PYB-SOs and PYB-SAs tested inhibited the formation of the EBI: β-tubulin adduct similarly to CA-4 and illustrated by the loss of the second immunoreacting band of β-tubulin and the presence of the native β-tubulin band [21]. These results show that both PYB-SO and PYB-SA derivatives bind efficiently to the C-BS leading to the depolymerisation of microtubules, disruption of the cytoskeleton and also the arrest of cell cycle progression in G<sub>2</sub>/M phase. This evidences the bioisosterism between 2-oxopyrrolidin-1-yl and the IMZ moieties of PIB-SOs and PIB-SAs and also that the nitrogen atom of the IMZ moiety is not involved in indispensable interactions in the C-BS.

### 3.6. PYB-SOs 14 and 15 and PYB-SAs 30 and 31 dock into the C-BS

In the aim to predict the active conformation of PYB-SOs and PYB-SAs and to identify the key amino acids involved in their interactions with the C-BS, molecular docking studies were performed to prepare a binding model derived from tubulin (protein data bank (PDB): 1SA0) [22] using the docking tool in the Molecular Operating Environment (MOE) software. The C-BS used to build our computational model is constituted of GTP and 32 amino acids distributed in the vicinity of the colchicine and GTP. The energy docking results of the 5 most favourable poses of PYB-SOs **14** and **15** and PYB-SAs **30** and **31** in the C-BS are shown in Table 2. Firstly, the

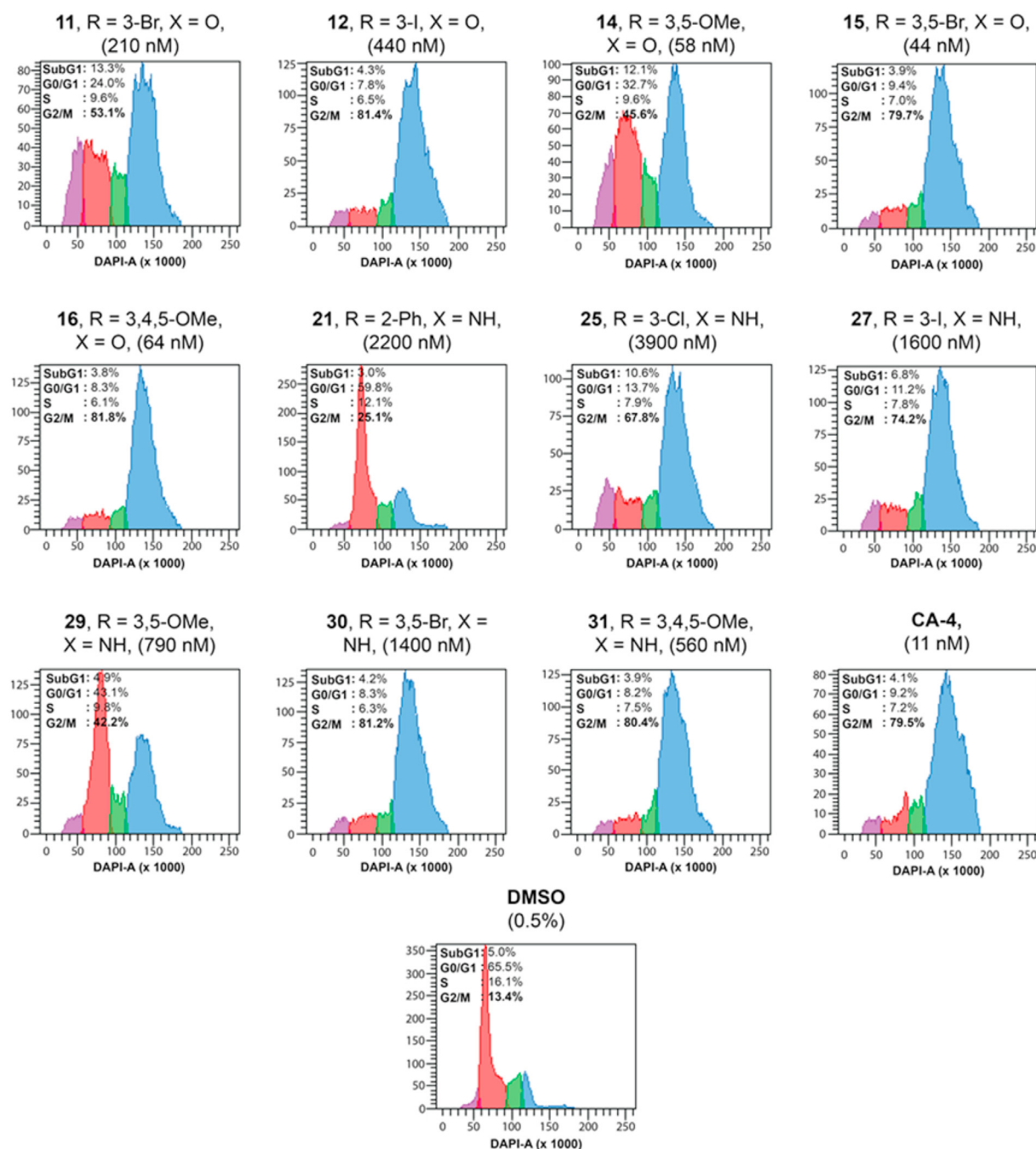


Fig. 2. Effect of PYB-SOs **11**, **12**, **14–16** and PYB-SAs **21**, **25**, **27**, **29–31** on the cell cycle progression of M21 cells after 24 h of treatment. CA-4 and DMSO were used as controls.

most favourable docking poses of PYB-SOs **14** and **15** and PYB-SAs **30** and **31** showing the lowest S-score ( $-7.49$ ,  $-7.29$ ,  $-7.08$  and  $-7.90$  kcal/mol, respectively) are depicted in Fig. 6. In addition, the superposition of these most favourable docking poses is illustrated in Fig. 7. Our results indicate that the molecular structure of selected PYB-SOs and PYB-SAs has the ability to dock into the C-BS. PYB-SO **14** and PYB-SA **30** are positioned into the C-BS similarly while PYB-SO **15** and PYB-SA **31** adopt different poses. Fig. 8 illustrates 2D interaction diagrams of the most favourable PYB-SO and PYB-SA poses and Table 3 summarises their key interactions with amino acids present into the C-BS. The aromatic ring B of compound **14** performs a pi-H interaction with Leu248, while compound **15** is generating two distinct H-donor interactions with

Ala317 and Val238, respectively through its bromine atoms and it also forms an H-acceptor interaction with Lys352 via its ketone moiety. In our model, the most favourable poses for PYB-SAs **30** and **31** are not driven by pi-H, hydrogen bonds or halogen bonds but driven by van der Waals interaction with the C-BS. These results indicate that both amino acids (Leu248, Ala317, Val238 and Lys352) and conformation poses are important for the interactions of PYB-SOs and PYB-SAs with the C-BS.

### 3.7. PYB-SOs and PYB-SAs have low to no toxicity toward chick embryos

The toxicity of the most potent PYB-SOs **14** and **15** and PYB-SAs

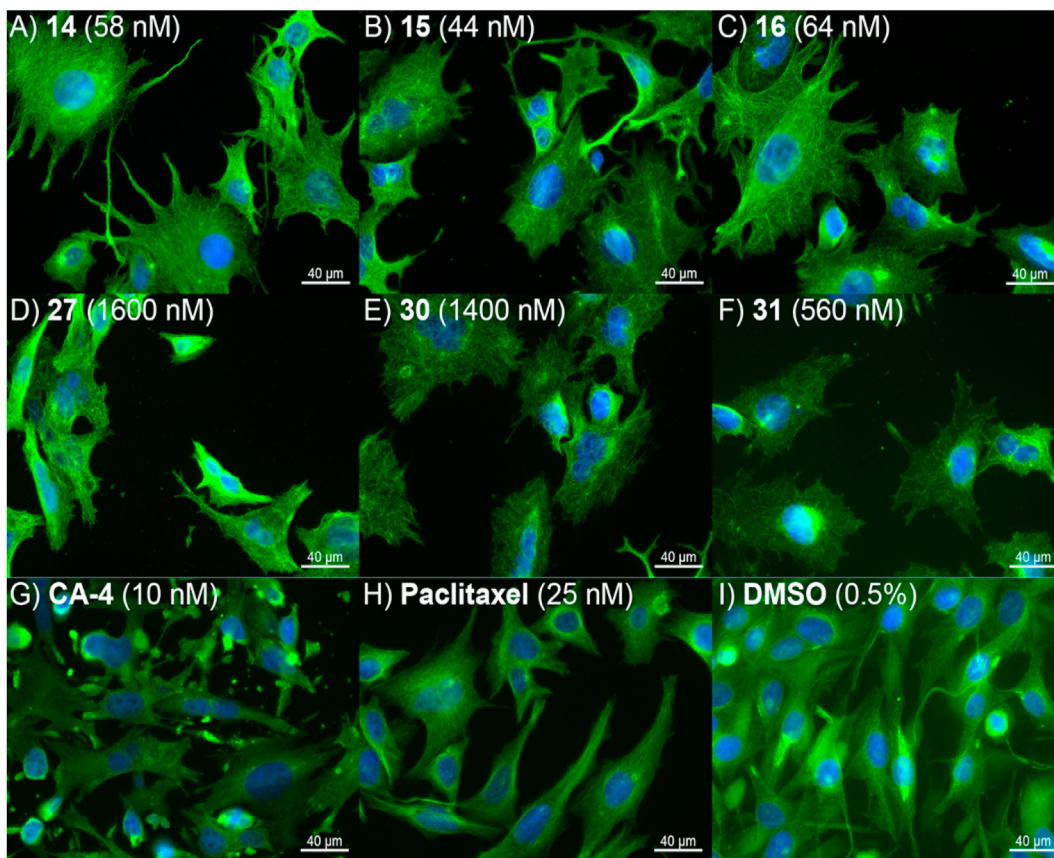


**Fig. 3.** Effect of PYB-SOs 14–16 and PYB-SAs 27, 30 and 31 on cytoskeleton integrity of M21 cells after 24 h of treatment (400-times total magnification). CA-4 and paclitaxel were used as positive controls while DMSO was used as negative control.

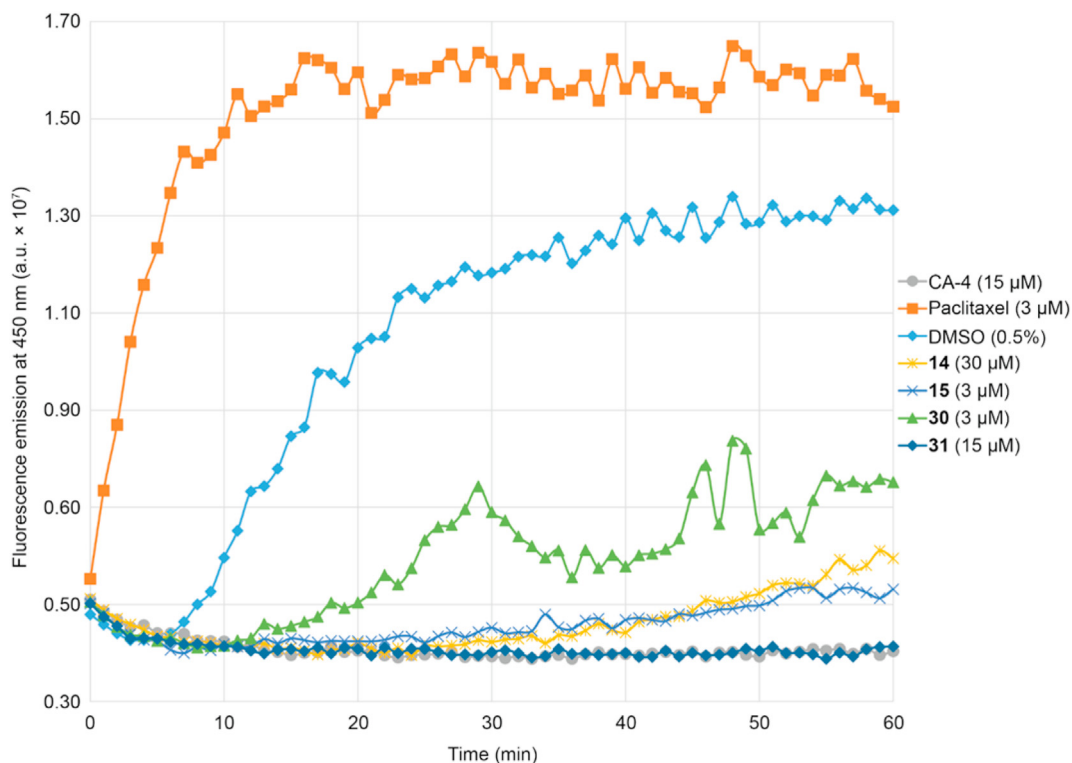


**Fig. 4.** Effect of PYB-SOs 14 and 15 and PYB-SAs 30 and 31 on tubulin assembly. CA-4 and paclitaxel were used as positive controls while DMSO was used as negative control.

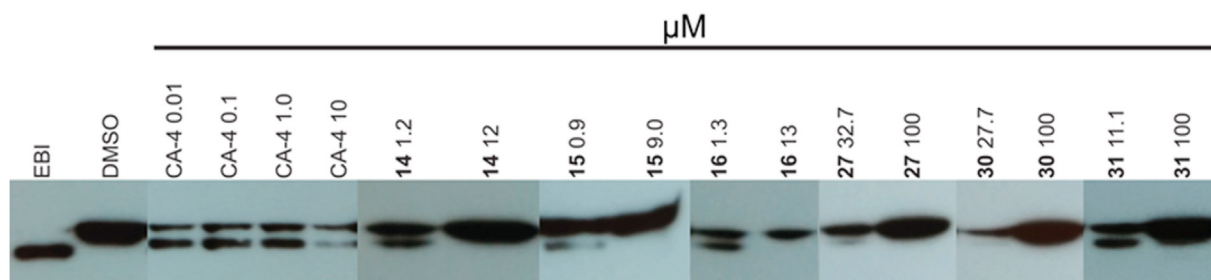


**Fig. 5.** Effect of PYB-SOs **14–16** and PYB-SAs **27, 30** and **31** on the binding of EBI to the colchicine-binding site at 100 and 1000-times their respective  $IC_{50}$ . CA-4 was used as positive control while DMSO and EBI were used as negative and positive controls, respectively.

**Table 2**

Docking energy scores of the 5 most favourable poses of PYB-SOs **14** and **15** and PYB-SAs **30** and **31** in the colchicine-binding site.

Pose	14		15		30		31	
	S (kcal/mol)	RMSD refine (Å)						
1	-7.49	1.13	-7.29	1.49	-7.08	1.19	-7.90	1.90
2	-7.30	1.79	-7.12	2.67	-7.05	0.91	-7.84	1.96
3	-7.25	2.02	-7.02	2.75	-6.86	2.08	-7.79	1.13
4	-7.23	1.03	-6.91	1.19	-6.79	1.77	-7.76	2.82
5	-7.04	1.85	-6.89	1.99	-6.78	1.56	-7.73	1.61

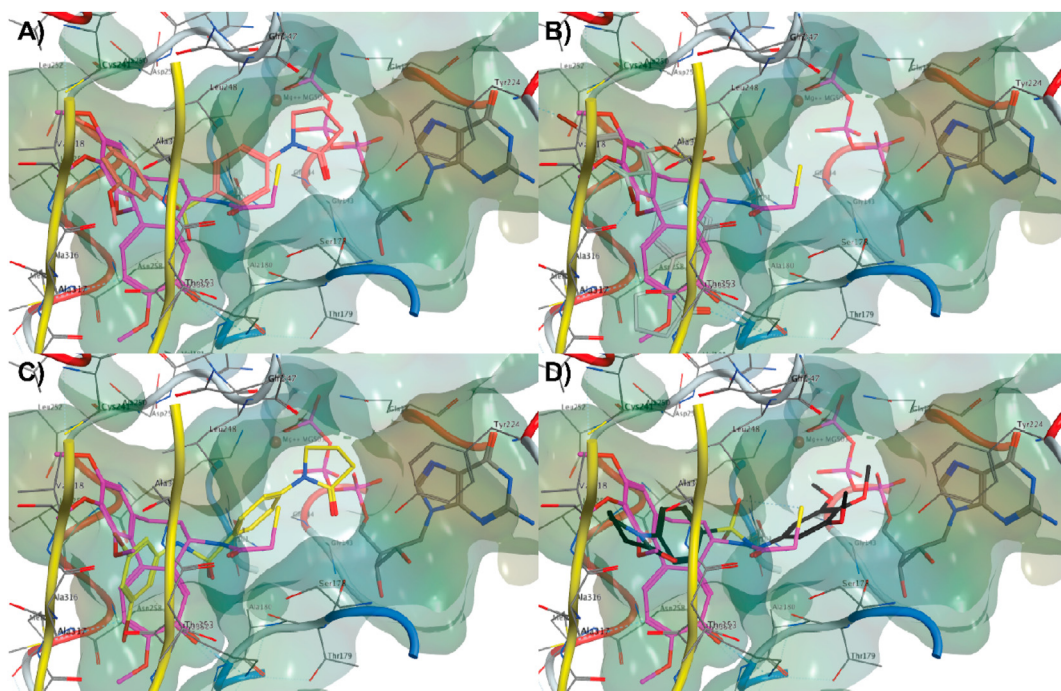


**Fig. 6.** Docking of the most stable poses of PYB-SOs and PYB-SAs superposed with colchicine (purple). A) **14** (red), B) **15** (white), C) **30** (yellow) and D) **31** (black) into the colchicine-binding site. (For interpretation of the references to color in this figure legend, the reader is referred to the Web version of this article.)

**30** and **31** was assessed on chick embryos. A mixture of 1.0% DMSO, 6.2% cremophor EL™, 6.2% ethanol (99%) and 86.6% PBS was used as excipient to administrate PYB-SOs **14** (20  $\mu\text{g}/\text{egg}$ ) and **15** (10  $\mu\text{g}/\text{egg}$ ) and PYB-SAs **30** (10  $\mu\text{g}/\text{egg}$ ) and **31** (1  $\mu\text{g}/\text{egg}$ ). A group of untreated chick embryos as well as another group of chick embryos that were exclusively treated with the excipients were used as negative controls. Drugs were injected at their maximum solubility in the formulation. The percentages of weight of different groups relative to the weight of untreated embryos are depicted in Fig. 9. First, the formulation is not toxic since there is no statistically

significant difference between the untreated and the excipient groups (100% vs 95%, F value of 0.58 compared to a critical F value of 4.11). Second, the percentage of weight of embryos treated by PYB-SOs **14** and **15** and PYB-SAs **30** and **31** relative to the weight of embryos untreated are 95, 93, 83 and 93%, respectively. Third, the percentage of death embryos of untreated, excipient, PYB-SOs **14** and **15** and PYB-SAs **30** and **31** are 17, 18, 18, 18, 25 and 8%, respectively. Although PYB-SA **30** has a lower percentage of embryos weight and a higher death rate, these percentage differences are not statistically significant with the excipient. Our results show

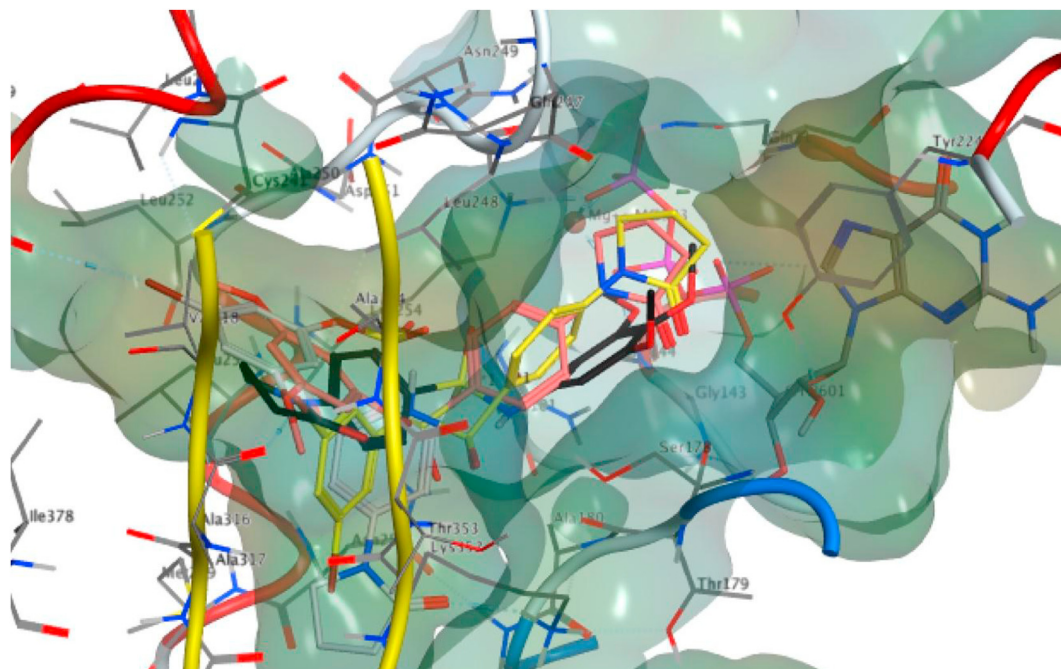


Fig. 7. Superposition of the docking of the most stable poses of PYB-SOs and PYB-SAs into the colchicine-binding site. Color coding: **14** (red), **15** (white), **30** (yellow) and **31** (black). (For interpretation of the references to color in this figure legend, the reader is referred to the Web version of this article.)

that PYB-SOs and PYB-SAs have very low to no toxicity toward chick embryos and present important features for the future development of this new family of antimicrotubule agents.

### 3.8. PYB-SOs and PYB-SAs have drug-like properties

Pharmacokinetics, physicochemical and drug-likeness properties are important in the development of new medicinal entities. To that end, we used the SwissADME free online tool to estimate the effect of structural modifications of our new PYB-SOs and PYB-SAs on their theoretical pharmacokinetics, physicochemical and drug-likeness properties [18]. PYB-SOs **11**, **12** and **14–16** and PYB-SAs **21**, **25**, **27** and **29–31** were selected for analysis and the results are summarised in Table 4. First, PYB-SOs and PYB-SAs have molecular weights ranging from 377.41 to 475.15 and 350.82–474.17 g/mol, respectively. The number of rotatable bonds varies from 4 to 7 for both classes of compounds. PYB-SO derivatives have 4 to 7 H-bond acceptors and 0 H-bond donor while PYB-SA derivatives have 3 to 6 H-bond acceptors and 1 H-bond donor. The topological polar surface area (TPSA) ranges from 72.06 to 99.75 and 74.86 to 102.55 Å<sup>2</sup> for PYB-SOs and PYB-SAs, respectively. The CLogP varies from 2.54 to 3.78 and 1.98 to 3.37 for PYB-SOs and PYB-SAs, respectively while LogS varies from −5.04 to −3.93 and −4.76 to −3.39. In general, compounds bearing a 3,5-dimethoxyl or a 3,4,5-trimethoxyl group are more soluble than their halogenated counterparts regardless of the presence of a sulfonate or a sulfonamide bridge. Globally, all compounds exhibit roughly similar ClogPs and LogSs and are either in the moderately soluble or soluble class. Moreover, all PYB-SOs and PYB-SAs evaluated so far have a high probability of gastrointestinal absorption (GIA). Beside compounds **11**, **12**, **25** and **27**, all PYB-SOs and PYB-SAs are predicted to be able to diffuse through the blood-brain barrier (BBB). PYB-SOs and PYB-SAs at the exception of compounds **29** and **31** should not be substrates of the p-glycoprotein, an efflux protein that is responsible for multidrug resistance. Of interest, PYB-SOs and PYB-SAs do not exhibit violation of either the Lipinski, Veber, Egan or

Muegge filters, which means that these compounds have the potential to be absorbed through the gastrointestinal tract. Therefore, PYB-SOs and PYB-SAs display high theoretical druglikeness properties and bioavailability scores despite chemical and structural modulations showing that PYB-SOs and PYB-SAs are promising for *in vivo* experiments.

## 4. Conclusion

In conclusion, we reported here the synthesis and the biological activity of 30 new PYB-SO and PYB-SA derivatives. They are active in the low nanomolar to the low micromolar levels on the four human cancer cell lines assessed. They arrest the cell cycle progression in G2/M phase, inhibit polymerisation of tubulin to microtubules, bind to the C-BS, and exhibit low to no toxicity toward chick embryos. In addition, as determined by the SwissADME algorithm they possess druglikeness properties and bioavailability scores suitable for *in vivo* experiments. Therefore, PYB-SOs and PYB-SAs are a new family of promising antimicrotubule agents.

## 5. Experimental protocols

### 5.1. Biological methods

#### 5.1.1. Cell lines culture

HT-1080 human fibrosarcoma, HT-29 human colon carcinoma, and MCF7 human breast carcinoma were purchased from the American Type Culture Collection (Manassa, VA, USA). M21 human skin melanoma cells were provided by Dr. David Cheresch (University of California, San Diego School of Medicine, CA). Cells were cultured in DMEM medium containing sodium bicarbonate, high glucose concentration, glutamine and sodium pyruvate (Hyclone, Logan, UT, USA) supplemented with either 5 or 10% of fetal bovine serum (FBS, Invitrogen, Burlington, ON, Canada) and were maintained at 37 °C in a moisture-saturated atmosphere containing 5% CO<sub>2</sub>.

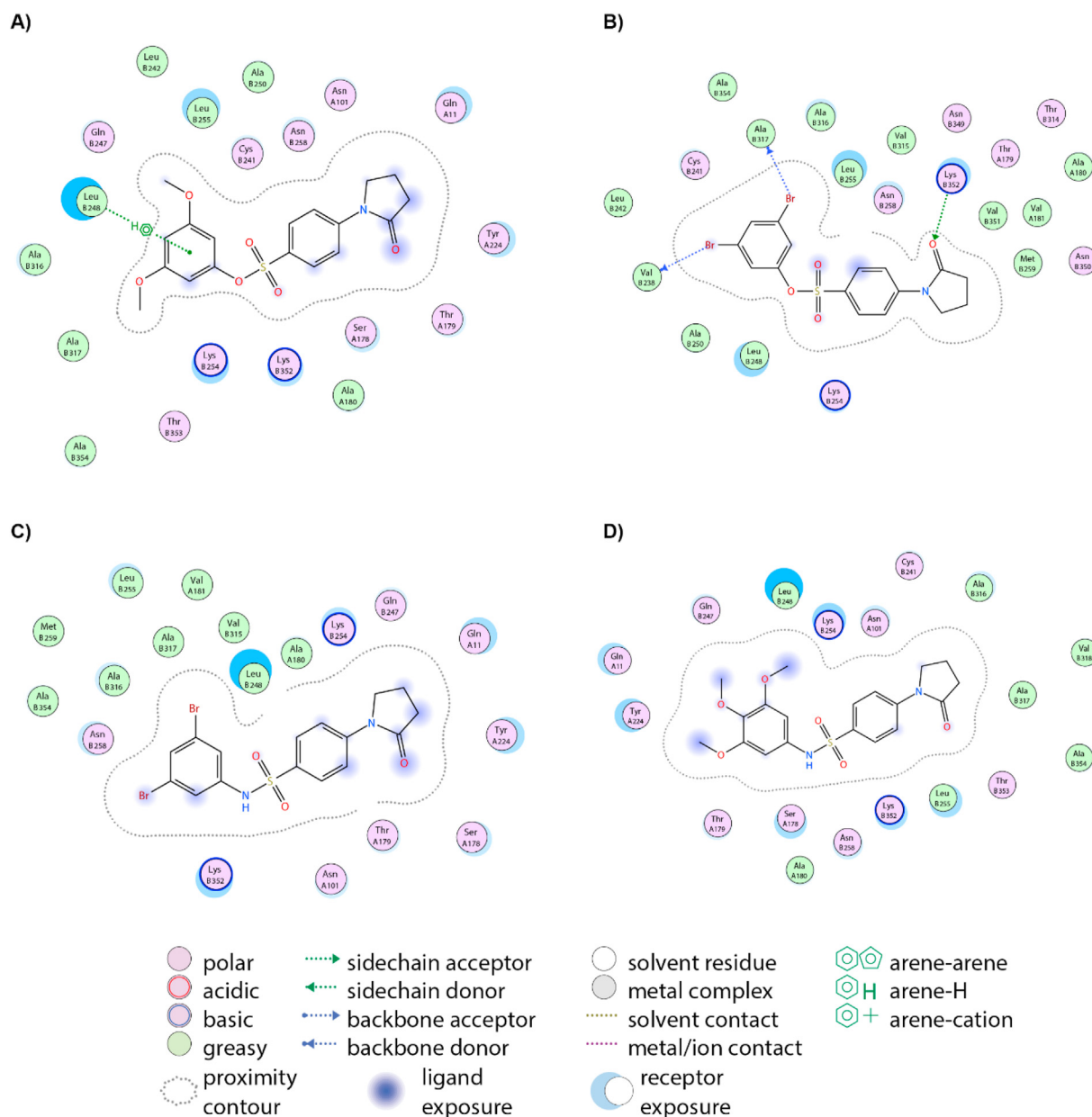


**Fig. 8.** 2D interaction diagrams of the most stable poses of PYB-SOs and PYB-SAs into the colchicine-binding site A) **14**, B) **15**, C) **30** and D) **31**.

**Table 3**

Interactions summary of PYB-SOs **14**, **15** and PYB-SAs **30** and **31** with the amino acids of the colchicine-binding site.

	Ligand		Receptor		Interaction		Distance (Å)	Energy (Kcal/mol)
	Atom	Atom	Atom	Atom	Amino Acid	Type		
<b>14</b>	6-ring	CD1	Leu248	pi-H	3.53	-0.5		
<b>15</b>	BR	O	Ala317	H-donor	3.50	-0.6		
	BR	O	Val238	H-donor	3.39	-1.5		
	O	NZ	Lys352	H-acceptor	3.20	-6.2		
<b>30</b>	—	—	—	—	—	—		
<b>31</b>	—	—	—	—	—	—		

### 5.1.2. Antiproliferative activity assay

The antiproliferative activity of PYB-SOs **4–18** and PYB-SAs **19–33** was assessed using the procedure described by the National Cancer Institute (NCI) Developmental Therapeutics Program

for its drug screening program with slight modifications [23]. Briefly, ninety-six-well Costar microtiter clear plates were seeded with 75  $\mu\text{L}$  of a suspension of either HT-1080 ( $2.5 \times 10^3$ ), HT-29 ( $4.0 \times 10^3$ ), M21 ( $3.0 \times 10^3$ ) or MCF7 ( $2.5 \times 10^3$ ) cells per well in DMEM supplemented with 5 or 10% FBS. Freshly solubilised drugs in DMSO (40 mM) were diluted in fresh supplemented DMEM and 75  $\mu\text{L}$  aliquots containing serially diluted concentrations of the drug were added. Final drug concentrations ranged from 100  $\mu\text{M}$  to 0.39 nM. DMSO concentration was kept constant at 0.5% (v/v) to prevent any related toxicity. Plates were incubated for 48 h, after which growth was stopped by the addition of cold trichloroacetic acid to the wells (10% w/v, final concentration). Afterwards, plates were incubated at 4  $^{\circ}\text{C}$  for 1 h. Then, plates were washed 5-times with distilled water and a sulforhodamine B solution (0.1% w/v) in 1% acetic acid was added to each well. After 15 min at room temperature, the exceeding dye was removed and the plates were washed 5-times with a solution of 1% acetic acid. Bound dye was solubilised in

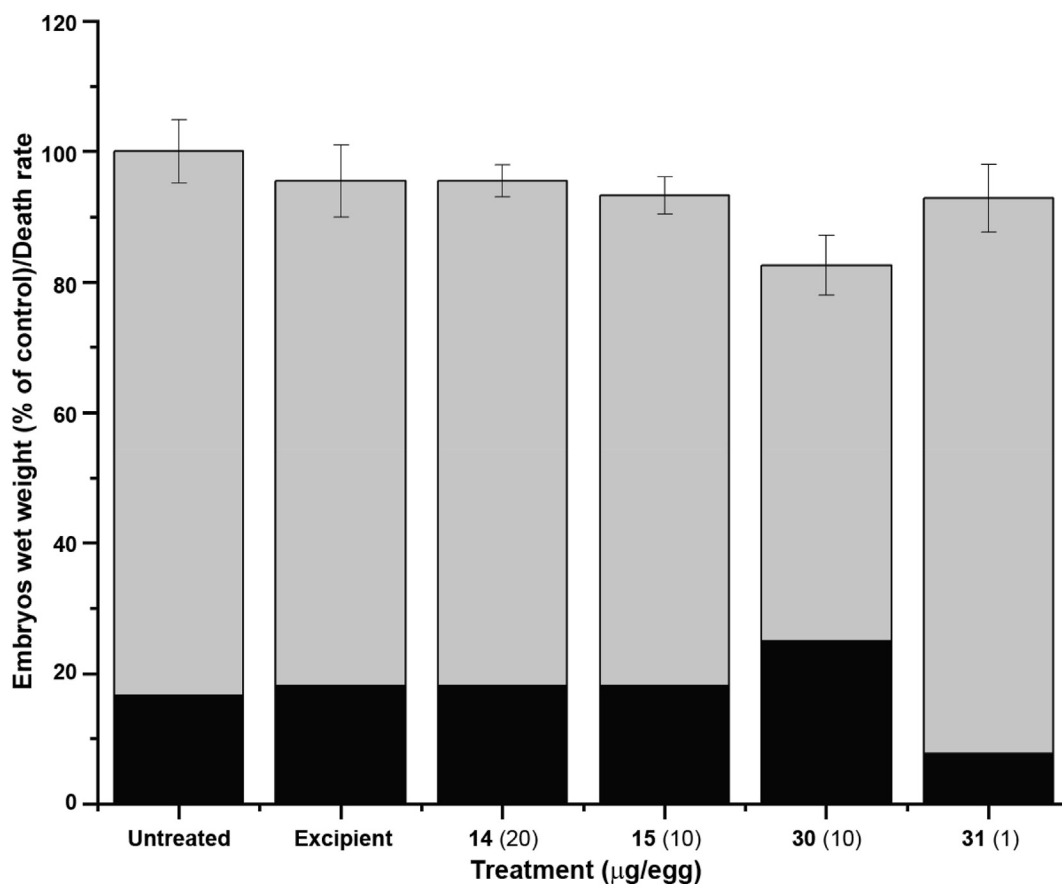


**Fig. 9.** Effect of PYB-SOs **14** and **15** and PYB-SAs **30** and **31** on the weight and the mortality of chick embryos. Grey bars represent the percentage of wet weight embryos relative to untreated wet weight embryos. Black bars represent the percentage of chick embryo mortality.

**Table 4**

Physicochemical properties, pharmacokinetic properties and druglikeness of PYB-SOs **11**, **12**, **14**–**16**, and PYB-SAs **21**, **25**, **27**, **29**–**31** calculated using the web-based SwissADME application.

#	Rb <sup>a</sup>	H-Ba <sup>b</sup>	H-BD <sup>c</sup>	TPSA <sup>d</sup> (Å <sup>2</sup> )	CLogP <sup>e</sup>	LogS <sup>f</sup>	Sclass <sup>g</sup>	GIA <sup>h</sup>	BBBP <sup>i</sup>	Pgp <sup>j</sup>	Drug-like (#viol.) <sup>k</sup>
<b>11</b>	4	4	0	72.06	3.15	−4.32	MS	H	Yes	No	Yes (0)
<b>12</b>	4	4	0	72.06	3.20	−4.27	MS	H	Yes	No	Yes (0)
<b>14</b>	6	6	0	90.52	2.56	−3.93	S	H	No	No	Yes (0)
<b>15</b>	4	4	0	72.06	3.78	−5.04	MS	H	No	No	Yes (0)
<b>16</b>	7	7	0	99.75	2.54	−4.09	MS	H	No	No	Yes (0)
<b>21</b>	5	3	1	74.86	3.37	−4.76	MS	H	No	No	Yes (0)
<b>25</b>	4	3	1	74.86	2.60	−3.72	S	H	Yes	No	Yes (0)
<b>27</b>	4	3	1	74.86	2.75	−3.74	S	H	Yes	No	Yes (0)
<b>29</b>	6	5	1	93.32	2.10	−3.39	S	H	No	Yes	Yes (0)
<b>30</b>	4	3	1	74.86	3.31	−4.50	MS	H	No	No	Yes (0)
<b>31</b>	7	6	1	102.55	1.98	−3.55	S	H	No	Yes	Yes (0)

<sup>a</sup> Rb: number of rotatable bonds.

<sup>b</sup> H-Ba: number of H-bond acceptors.

<sup>c</sup> H-BD: number of H-bond donors.

<sup>d</sup> TPSA: topological polar surface area.

<sup>e</sup> CLogP: consensus Log P (average of iLOGP, XLOGP3, WLOGP, MLOGP and Silicos-IT Log P).

<sup>f</sup> LogS: Ali topological method Log S.

<sup>g</sup> SClass: Ali solubility class (insoluble (IS) < −10 < poorly soluble (PS) < −6 < moderately soluble (MS) < −4 < soluble (S) < −2 < very soluble (VS) < 0 < highly soluble (HS)).

<sup>h</sup> GIA: gastrointestinal absorption (H means high).

<sup>i</sup> BBBP: blood-brain barrier permeability.

<sup>j</sup> Pgp: p-glycoprotein substrates.

<sup>k</sup> Drug-like: drug-likeness indices (bioavailability) from Lipinski, Ghose, Veber, Egan and Muegge filters. # viol: number of violations of the 5 filters.

20 mM Tris base and the absorbance was read using an optimal wavelength (520–580 nm) with a SpectraMax® i3x (Molecular Devices, San Jose, CA, USA). Data obtained from treated cells were compared to the control cell plates fixed on the treatment day and

the percentage of cell growth was thus calculated for each drug. The experiments were done at least twice in triplicate. The assays were considered valid when the coefficient of variation was <10% for a given set of conditions within the same experiment.

### 5.1.3. Cell cycle progression analysis

After incubation of  $2.5 \times 10^5$  M21 cells with selected PYB-SOs and PYB-SAs at 2- and 5-times their respective  $IC_{50}$  for 24 h, the cells were trypsinised, washed with 750  $\mu$ L of phosphate buffered saline (PBS) and resuspended in 250  $\mu$ L of PBS. Cells were fixed by the addition of 750  $\mu$ L of ice-cold ethanol under agitation and stored at  $-20^\circ\text{C}$  until analysis. Prior analysis, cells were washed with 750  $\mu$ L of PBS and resuspended in 300  $\mu$ L of PBS containing 2  $\mu$ g/mL DAPI. Cell cycle distribution of fixed cell suspensions was analysed using an LSR II flow cytometer (BD Biosciences, Franklin Lakes, NJ, USA).

### 5.1.4. Immunofluorescence of microtubules

MCF7 cells were seeded at  $2.5 \times 10^5$  cells per well in 6-well plates (Costar®) containing glass cover slides (22 mm  $\times$  22 mm) coated with fibronectin (10  $\mu$ g/mL) and incubated for 24 h. Tumour cells were treated either with PYB-SOs **14** (58 nM) and **15** (44 nM), PYB-SAs **30** (1400 nM) and **31** (560 nM), paclitaxel (25 nM) or CA-4 (10 nM) for 24 h. DMSO (0.5%) was used as negative control while paclitaxel and CA-4 were used as positive controls. The cells were then washed thrice with 2 mL of PBS and fixed with 3.7% formaldehyde in PBS for 10 min. After two washes with PBS, the cells were permeabilised with saponin (0.1% in PBS) and blocked with 3% (w/v) BSA in PBS for 45 min at  $37^\circ\text{C}$ . The cells were then incubated for 2 h at room temperature with an anti- $\beta$ -tubulin monoclonal antibody (clone TUB 2.1, 1:300) in a solution containing 0.1% saponin and 3% BSA in PBS. The cells were washed thrice with PBS containing 0.05% Tween 20 and stained using antimouse IgG Alexa Fluor 488 (Molecular Probes, Eugene, OR, USA; 1:1000) and DAPI (1.25 ng/mL final concentration) in blocking buffer for 1 h at  $37^\circ\text{C}$ . The cover slides were mounted using 25  $\mu$ L of Fluoromount-G® (SouthernBiotech, Birmingham, AL, USA) before analysis under an Olympus BX51 fluorescence microscope (Olympus BX51, Center Valley, PA, USA). Images were acquired as 8 bit-tagged image format files with a Q imaging RETIGA EXI digital camera (Qimaging, Surrey, BC, Canada) using the Image Pro Express software at a total magnification of  $400\times$ .

### 5.1.5. Microtubule polymerisation assay

The effect of PYB-SOs **14** (30  $\mu$ M) and **15** (3  $\mu$ M) and PYB-SAs **30** (3  $\mu$ M) and **31** (15  $\mu$ M) on dynamic polymerisation of tubulin to microtubules was analysed with the fluorescence based Tubulin polymerisation assay using >99% pure tubulin (Cytoskeleton, Inc., Denver, CO, USA). Drugs were solubilised at the required concentration in DMSO, then 5  $\mu$ L of drug solutions were diluted in 325  $\mu$ L of nanopure water to reach 10x of their final concentration. The assay was performed according to the manufacturer guidelines [24]. Briefly, tubulin >99% (2.0 mg/mL) was dissolved in general tubulin buffer (80 mM PIPES pH 6.9, 0.5 mM EGTA, 2.0 mM  $MgCl_2$ ) and incubated with drugs at  $37^\circ\text{C}$ . The polymerisation was measured over 60 min with fluorescent excitation at 360 nm and emission at 450 nm in kinetic mode with a SpectraMax® i3x (Molecular Devices, San Jose, CA, USA). The curves shown in Fig. 8 are representative of 2 separated experiments.

### 5.1.6. In vitro competition binding assay of EBI to the C-BS

M21 cells were seeded at a concentration of  $7.5 \times 10^5$  M21 cells/well and were incubated overnight in 6-well plates. Then, cells were treated with either PYB-SOs **14** and **15** or PYB-SAs **30** and **31** for 1.5 h at 100- and 1000-times their respective  $IC_{50}$  for 2 h. The maximum concentration of PYB-SOs and PYB-SAs used for the experiments was set at 100  $\mu$ M. Next, 100  $\mu$ L of EBI (100  $\mu$ M, final concentration, Toronto Research Chemicals, North York, ON, Canada) in PBS were added to each well for 1.5 h. After the incubation, the supernatant was withdrawn and the cells in the plates were

trypsinised (trypsin-EDTA 0.5%), harvested and centrifuged for 5 min at 1200 rpm. The pellets were washed with 500  $\mu$ L by cold PBS and stored at  $-80^\circ\text{C}$  until analysis.

### 5.1.7. Gel electrophoresis and immunoblot

The cell pellets were resuspended in a buffer containing 0.32 M sucrose, 1 mM EDTA at pH 8, 10 mM Tris at pH 7.4 and protease inhibitor. The protein concentration was assessed using the Bio-Rad protein assay (Bio-Rad laboratories, Mississauga, ON, Canada). Samples were prepared and diluted to obtain proteins at 4 mg/mL in Laemmli sample buffer [25] (60 mM Tris-Cl at pH 6.8, 2% SDS, 10% glycerol, 5%  $\beta$ -mercaptoethanol, 0.01% bromophenol blue) and boiled for 5 min. Then, 40  $\mu$ g of proteins from the protein extracts were used for the electrophoresis using 10% polyacrylamide gels. The proteins were transferred onto nitrocellulose membranes that were incubated with TBSTM (Tris-Buffered Saline + 0.1% (v/v) Tween-20 with 5% fat-free dry milk) for 2 h at room temperature. Next, the anti- $\beta$ -tubulin (clone TUB 2.1, Sigma-Aldrich, St. Louis, MO, USA) primary antibody was incubated in TBSTM (1:500) for 2 h at room temperature. Membranes were washed with TBST (Tris-Buffered Saline with 0.1% (v/v) Tween 20) and incubated with peroxidase conjugated anti-mouse immunoglobulin (Amersham Canada, Oakville, ON, Canada) in TBSTM (1:5000) for 1 h at room temperature. After washing the membranes with TBST, detection of the immunoblot was carried out using Clarity Western enhanced chemiluminescence reagents (Bio-Rad laboratories, Mississauga, ON, Canada). Detection of bands was performed with Super Rx medical X-Ray film (Fujifilm, Tokyo, Japan).

### 5.1.8. Toxicity toward chick embryos

Fertilised eggs were purchased from Couvoir La Coop (Victorville, QC, Canada). They were incubated for a 10-days period in a Pro-FI egg incubator (Lyon Electric, Chula Vista, CA, USA) with an automatic turning system. Compounds were solubilised in a formulation containing 1.0% DMSO, 6.2% cremophor EL™, 6.2% ethanol (99%) and 86.6% PBS. After the incubation period, the veins of the chorioallantoic membrane were identified on the sides of the egg shells. The eggs were opened using a hobby drill (Dremel, Racine, WI) to obtain a  $1.5 \times 1.5$  cm opening directly over the location of the veins. Groups of 10–12 eggs were formed by randomisation and the drugs were intravenously administered at their maximum solubility in our excipient (100  $\mu$ L/egg). The openings were closed using adhesive tape and the eggs were then incubated in a static incubator (Lyon Electric, Chula Vista, CA, USA) for a 7-days period at  $37^\circ\text{C}$ . The embryos were euthanised at  $4^\circ\text{C}$  for at least 2h. The wet weight of each embryo and the number of dead embryos were registered. A group of untreated embryos and a group of embryos that were treated only with the excipient were used as negative controls. A one-way ANOVA analysis was used to determine the statistical significance of the results.

## 5.2. Chemical methods

### 5.2.1. General

Proton NMR spectra were recorded on a Bruker AM-300 spectrometer (Bruker, Germany). Chemical shifts ( $\delta$ ) are reported in parts per million (ppm). Reactions requiring microwave heating were performed at 200 W with an initiator system (Biotage, Charlottesville, VA, USA). Uncorrected melting points were obtained on a MPA100 automated melting point system (SRS Stanford Research Systems, Sunnyvale, CA, USA). UHPLC analyses were performed using an ACQUITY Arc system (Waters, Mississauga, ON, Canada) equipped with a 2998 PDA detector. The samples were obtained by solubilisation of the compounds in DMSO and a subsequent solution was produced by diluting the compounds at 1%

DMSO in a mixture of MeOH/H<sub>2</sub>O 50:50. These samples were then eluted using a mixture of MeOH/H<sub>2</sub>O with a linear mobile phase gradient (1.0 mL/min) on a CORTECS C18+ reversed-phase column 3.0 × 50 mm × 2.7 μm (Waters, Mississauga, ON, Canada). Wavelength was selected at 280 nm and the percentage of all the present compounds was determined. Purity was confirmed by UHPLC and was equal or greater than 95%. All chemicals were supplied by Aldrich Chemicals (Milwaukee, WI, USA), VWR International (Mont-Royal, QC, Canada), Fisher Scientific (Montreal, QC, Canada). Liquid flash chromatography was performed on silica gel F60, 60 Å, 40–63 μm supplied by Silicycle (Quebec, QC, Canada) using an FPX flash purification system (Biotage, Charlottesville, VA, USA), and using solvent mixtures expressed as v/v ratios. Solvents and reagents were used without purification unless specified otherwise. The progress of all reactions was monitored by TLC on precoated silica gel 60 Å F254 TLC plates provided by VWR International (Mont-Royal, QC, Canada). The chromatograms were viewed under UV light at 254 and/or 275 nm. HRMS were recorded by direct injection in a TOF system 6210 series mass spectrometer (Agilent technologies, Santa Clara, CA, USA).

### 5.2.2. Preparation of compound 34

4-Chlorobutanoyl chloride (6.1 mL, 1.0 Eq) was added to a solution of aniline (5.0 mL, 1.0 Eq) in methylene chloride (100 mL) in presence of triethylamine (9.2 mL, 1.2 Eq). The reaction mixture was stirred at room temperature for 24 h. After completion of the reaction, the mixture was washed twice with HCl 1M (100 mL) and brine (100 mL). The resulting organic solution was dried over anhydrous sodium sulfate, filtered and evaporated to dryness under reduced pressure. The product 4-chloro-*N*-phenylbutanamide (**34**) was used without further purification with a yield of 86%. The <sup>1</sup>H and <sup>13</sup>C NMR are equivalent to the NMR characterisation published previously [26].

### 5.2.3. Preparation of compound 35

Compound **35** was prepared as published previously with slight modifications [27]. Briefly, sodium hydride (in oil [60%], 2.2 g, 1.2 Eq) was dissolved in an ice-cold solution of 4-chloro-*N*-phenylbutanamide (**34**, 9.0 g, 1.0 Eq) in dry THF (250 mL) under argon atmosphere. The ice bath was removed after 10 min. The reaction was stirred at room temperature for 24 h. The reaction was quenched at 0 °C with water (50 mL) and the organic solvent was evaporated. The aqueous solution was extracted with AcOEt (250 mL). The organic solution washed twice with brine (250 mL), dried over anhydrous sodium sulfate, filtered and evaporated to dryness under reduced pressure. The residue was purified by flash chromatography on silica gel (hexanes/AcOEt (75:25) to hexanes/AcOEt (66:33) to obtain 1-phenylpyrrolidin-2-one (**35**) with a yield of 78%. The <sup>1</sup>H and <sup>13</sup>C NMR are equivalent to the NMR characterisation published previously [28].

### 5.2.4. Preparation of compound 36

Compound **36** was prepared as published previously with slight modifications [29]. Briefly, 1-phenylpyrrolidin-2-one (**35**, 5.0 g, 1.0 Eq) was dissolved in ice cold chlorosulfonic acid (2.1 mL, 7.7 Eq) under a dry argon atmosphere. The ice bath was removed after 15 min. The reaction mixture was stirred at room temperature for 16 h. After completion of the reaction, the solution was poured on iced water dropwise. The solid was filtered, rinsed with water (100 mL) and dried for 1 h under vacuum. The resulting white 4-(2-oxopyrrolidin-1-yl)benzenesulfonyl chloride (**36**) was used without further purification with a yield of 72%.

### 5.2.5. General preparation of compounds 4–18

The relevant phenol (1.5 Eq) was added to a solution of the 4-(2-

oxopyrrolidin-1-yl)benzenesulfonyl chloride (**36**, 0.10 g) in acetonitrile (3.0 mL) in presence of triethylamine (0.16 mL, 3.0 Eq). The reaction mixture was stirred at 120 °C under microwave radiation for 8 h. After completion of the reaction, the mixture was cooled at room temperature and the solvent was evaporated under reduced pressure. The residue was diluted within AcOEt (10 mL) and was washed twice with HCl 1M (10 mL), NaOH 1M (10 mL) and brine (10 mL). The resulting solution was dried over anhydrous sodium sulfate, filtered and evaporated to dryness under reduced pressure. The residue was purified by flash chromatography on silica gel.

### 5.2.6. Characterization of compounds 4–18

**5.2.6.1. Phenyl 4-(2-oxopyrrolidin-1-yl)benzenesulfonate (4).** Flash chromatography (methylene chloride to methylene chloride/ethyl acetate (95:5)). Purity: 100.0%; yield: 83%; white solid; mp: 133–135 °C; <sup>1</sup>H NMR (CDCl<sub>3</sub>): δ 7.82–7.72 (m, 4H, Ar), 7.28–7.21 (m, 3H, Ar), 6.96–6.93 (m, 2H, Ar), 3.86 (t, 2H, *J* = 7.0 Hz, CH<sub>2</sub>), 2.63 (t, 2H, *J* = 8.0 Hz, CH<sub>2</sub>), 2.23–2.13 (m, 2H, CH<sub>2</sub>); <sup>13</sup>C NMR (CDCl<sub>3</sub>): δ 175.0, 149.6, 144.5, 129.7, 129.5, 129.4, 127.2, 122.3, 118.7, 48.3, 32.9, 17.7; HRMS (ESI) *m/z* found, 318.0802; C<sub>16</sub>H<sub>16</sub>NO<sub>4</sub>S (M<sup>+</sup> + H) expected, 318.0801.

**5.2.6.2. 2-Isopropylphenyl 4-(2-oxopyrrolidin-1-yl)benzenesulfonate (5).** Flash chromatography (hexanes/methylene chloride (50:50) to methylene chloride). Purity: 99.7%; yield: 61%; white solid; mp: 127–129 °C; <sup>1</sup>H NMR (CDCl<sub>3</sub>): δ 7.84 (brs, 4H, Ar), 7.27–7.18 (m, 2H, Ar), 7.12–7.07 (m, 1H, Ar), 7.01–6.98 (m, 1H, Ar), 3.89 (t, 2H, *J* = 7.0 Hz, CH<sub>2</sub>), 3.16–3.10 (m, 1H, CH), 2.66 (t, 2H, *J* = 8.0 Hz, CH<sub>2</sub>), 2.26–2.16 (m, 2H, CH<sub>2</sub>), 1.07 (d, 6H, *J* = 6.9 Hz, CH<sub>3</sub>); <sup>13</sup>C NMR (CDCl<sub>3</sub>): δ 174.9, 147.0, 144.4, 141.8, 130.5, 129.4, 127.3, 127.2, 126.7, 121.9, 118.8, 48.4, 32.8, 26.7, 23.1, 17.7; HRMS (ESI) *m/z* found, 360.1269; C<sub>19</sub>H<sub>22</sub>NO<sub>4</sub>S (M<sup>+</sup> + H) expected, 360.1269.

**5.2.6.3. [1,1'-Biphenyl]-2-yl 4-(2-oxopyrrolidin-1-yl)benzenesulfonate (6).** Flash chromatography (methylene chloride). Purity: 96.5%; yield: 97%; white solid; mp: 157–159 °C; <sup>1</sup>H NMR (acetone-*d*<sub>6</sub>): δ 7.66–7.64 (m, 2H, Ar), 7.47–7.13 (m, 11H, Ar), 3.94 (t, 2H, *J* = 6.9 Hz, CH<sub>2</sub>), 2.59 (t, 2H, *J* = 7.9 Hz, CH<sub>2</sub>), 2.26–2.16 (m, 2H, CH<sub>2</sub>); <sup>13</sup>C NMR (acetone-*d*<sub>6</sub>): δ 179.9, 151.7, 150.1, 141.8, 140.6, 136.4, 134.3, 134.3, 133.9, 133.9, 133.3, 132.8, 132.6, 129.0, 123.5, 53.2, 37.6, 22.7; HRMS (ESI) *m/z* found, 394.1110; C<sub>22</sub>H<sub>20</sub>NO<sub>4</sub>S (M<sup>+</sup> + H) expected, 394.1109.

**5.2.6.4. 2-Methoxyphenyl 4-(2-oxopyrrolidin-1-yl)benzenesulfonate (7).** Flash chromatography (methylene chloride to methylene chloride/ethyl acetate (97:3)). Purity: 96.5%; yield: 70%; white solid; mp: 157–158 °C; <sup>1</sup>H NMR (CDCl<sub>3</sub>): δ 7.83–7.76 (m, 4H, Ar), 7.20–7.11 (m, 2H, Ar), 6.89–6.81 (m, 2H, Ar), 3.88 (t, 2H, *J* = 7.0 Hz, CH<sub>2</sub>), 3.55 (s, 3H, CH<sub>3</sub>), 2.64 (t, 2H, *J* = 8.1 Hz, CH<sub>2</sub>), 2.24–2.14 (m, 2H, CH<sub>2</sub>); <sup>13</sup>C NMR (CDCl<sub>3</sub>): δ 174.9, 151.8, 144.3, 138.3, 130.5, 129.6, 128.1, 123.9, 120.6, 118.5, 112.7, 55.6, 48.4, 32.8, 17.7; HRMS (ESI) *m/z* found, 348.0902; C<sub>17</sub>H<sub>18</sub>NO<sub>5</sub>S (M<sup>+</sup> + H) expected, 348.0906.

**5.2.6.5. 3-Methoxyphenyl 4-(2-oxopyrrolidin-1-yl)benzenesulfonate (8).** Flash chromatography (methylene chloride/ethyl acetate (97:3)). Purity: 99.6%; yield: 71%; pale solid; mp: 122–124 °C; <sup>1</sup>H NMR (CDCl<sub>3</sub>): δ 7.83–7.76 (m, 4H, Ar), 7.16–7.11 (m, 1H, Ar), 6.77–6.74 (m, 1H, Ar), 6.56–6.50 (m, 2H, Ar), 3.87 (t, 2H, *J* = 7.0 Hz, CH<sub>2</sub>), 3.70 (s, 3H, CH<sub>3</sub>), 2.64 (t, 2H, *J* = 8.0 Hz, CH<sub>2</sub>), 2.24–2.14 (m, 2H, CH<sub>2</sub>); <sup>13</sup>C NMR (CDCl<sub>3</sub>): δ 175.0, 160.4, 150.4, 144.5, 129.9, 129.5, 129.5, 118.7, 114.2, 113.0, 108.3, 55.5, 48.4, 32.8, 17.7; HRMS (ESI) *m/z* found, 348.0899; C<sub>17</sub>H<sub>18</sub>NO<sub>5</sub>S (M<sup>+</sup> + H) expected, 348.0906.

**5.2.6.6. 3-Fluorophenyl 4-(2-oxopyrrolidin-1-yl)benzenesulfonate (9).** Flash chromatography (methylene chloride). Purity: 99.8%;

yield: 60%; white solid; mp: 120–122 °C;  $^1\text{H}$  NMR ( $\text{CDCl}_3$ ):  $\delta$  7.86–7.77 (m, 4H, Ar), 7.28–7.20 (m, 1H, Ar), 6.99–6.93 (m, 1H, Ar), 6.80–6.74 (m, 2H, Ar), 3.89 (t, 2H,  $J = 7.0$  Hz,  $\text{CH}_2$ ), 2.66 (t, 2H,  $J = 8.0$  Hz,  $\text{CH}_2$ ), 2.26–2.16 (m, 2H,  $\text{CH}_2$ );  $^{13}\text{C}$  NMR ( $\text{CDCl}_3$ ):  $\delta$  175.0, 164.3, 161.0, 150.2, 150.1, 144.7, 130.5, 130.4, 129.5, 129.2, 118.8, 118.2, 118.1, 114.5, 114.2, 110.6, 110.3, 48.3, 32.8, 17.7; HRMS (ESI)  $m/z$  found, 336.0696;  $\text{C}_{16}\text{H}_{15}\text{FNO}_4\text{S}$  ( $\text{M}^+ + \text{H}$ ) expected, 336.0707.

**5.2.6.7. 3-Chlorophenyl 4-(2-oxopyrrolidin-1-yl)benzenesulfonate (10).** Flash chromatography (methylene chloride/ethyl acetate (99:1) to (95:5)). Purity: 100.0%; yield: 79%; white solid; mp: 102–104 °C;  $^1\text{H}$  NMR ( $\text{CDCl}_3$ ):  $\delta$  7.85–7.76 (m, 4H, Ar), 7.26–7.16 (m, 2H, Ar), 7.04 (brs, 1H, Ar), 6.87–6.84 (m, 1H, Ar), 3.88 (t, 2H,  $J = 7.0$  Hz,  $\text{CH}_2$ ), 2.65 (t, 2H,  $J = 8.0$  Hz,  $\text{CH}_2$ ), 2.25–2.15 (m, 2H,  $\text{CH}_2$ );  $^{13}\text{C}$  NMR ( $\text{CDCl}_3$ ):  $\delta$  175.0, 149.9, 144.8, 134.9, 130.4, 129.5, 129.1, 127.5, 123.0, 120.6, 118.8, 48.3, 32.8, 17.7; HRMS (ESI)  $m/z$  found, 352.0393;  $\text{C}_{16}\text{H}_{15}\text{ClNO}_4\text{S}$  ( $\text{M}^+ + \text{H}$ ) expected, 352.0411.

**5.2.6.8. 3-Bromophenyl 4-(2-oxopyrrolidin-1-yl)benzenesulfonate (11).** Flash chromatography (methylene chloride/ethyl acetate (99:1) to (95:5)). Purity: 99.5%; yield: 74%; white solid; mp: 89–92 °C;  $^1\text{H}$  NMR ( $\text{CDCl}_3$ ):  $\delta$  7.85–7.76 (m, 4H, Ar), 7.38–7.35 (m, 1H, Ar), 7.20–7.11 (m, 2H, Ar), 6.91–6.88 (m, 1H, Ar), 3.88 (t, 2H,  $J = 7.0$  Hz,  $\text{CH}_2$ ), 2.65 (t, 2H,  $J = 8.0$  Hz,  $\text{CH}_2$ ), 2.25–2.15 (m, 2H,  $\text{CH}_2$ );  $^{13}\text{C}$  NMR ( $\text{CDCl}_3$ ):  $\delta$  175.0, 149.9, 144.8, 130.7, 130.4, 129.5, 129.1, 125.8, 122.5, 121.1, 118.8, 48.3, 32.8, 17.7; HRMS (ESI)  $m/z$  found, 395.9898;  $\text{C}_{16}\text{H}_{15}\text{BrNO}_4\text{S}$  ( $\text{M}^+ + \text{H}$ ) expected, 395.9906.

**5.2.6.9. 3-Iodophenyl 4-(2-oxopyrrolidin-1-yl)benzenesulfonate (12).** Flash chromatography (methylene chloride to methylene chloride/ethyl acetate (95:5)). Purity: 97.6%; yield: 31%; white solid; mp: 103–105 °C;  $^1\text{H}$  NMR ( $\text{CDCl}_3$ ):  $\delta$  7.86–7.77 (m, 4H, Ar), 7.59–7.56 (m, 1H, Ar), 7.38 (s, 1H, Ar), 7.03–6.92 (m, 2H, Ar), 3.90 (t, 2H,  $J = 7.0$  Hz,  $\text{CH}_2$ ), 2.66 (t, 2H,  $J = 8.0$  Hz,  $\text{CH}_2$ ), 2.26–2.16 (m, 2H,  $\text{CH}_2$ );  $^{13}\text{C}$  NMR ( $\text{CDCl}_3$ ):  $\delta$  175.0, 149.6, 144.7, 136.3, 131.5, 130.9, 129.6, 129.2, 121.7, 118.8, 93.5, 48.4, 32.8, 17.7; HRMS (ESI)  $m/z$  found, 443.9757;  $\text{C}_{16}\text{H}_{15}\text{INO}_4\text{S}$  ( $\text{M}^+ + \text{H}$ ) expected, 443.9767.

**5.2.6.10. 3,4-Dimethoxyphenyl 4-(2-oxopyrrolidin-1-yl)benzenesulfonate (13).** Flash chromatography (methylene chloride/ethyl acetate (97:3) to (95:5)). Purity: 97.6%; yield: 55%; white solid; mp: 152–153 °C;  $^1\text{H}$  NMR ( $\text{CDCl}_3$ ):  $\delta$  7.85–7.78 (m, 4H, Ar), 6.71–6.44 (m, 3H, Ar), 3.90 (t, 2H,  $J = 7.0$  Hz, Ar), 3.84 (s, 3H,  $\text{CH}_3$ ), 3.77 (s, 3H,  $\text{CH}_3$ ), 2.67 (t, 2H,  $J = 8.0$  Hz,  $\text{CH}_2$ ), 2.27–2.17 (m, 2H,  $\text{CH}_2$ );  $^{13}\text{C}$  NMR ( $\text{CDCl}_3$ ):  $\delta$  175.0, 149.3, 147.9, 144.5, 143.1, 129.7, 129.5, 118.7, 113.8, 110.7, 106.5, 56.1, 56.1, 48.4, 32.9, 17.8; HRMS (ESI)  $m/z$  found, 378.0991;  $\text{C}_{18}\text{H}_{20}\text{NO}_6\text{S}$  ( $\text{M}^+ + \text{H}$ ) expected, 378.1012.

**5.2.6.11. 3,5-Dimethoxyphenyl 4-(2-oxopyrrolidin-1-yl)benzenesulfonate (14).** Flash chromatography (methylene chloride to methylene chloride/ethyl acetate (97:3)). Purity: 99.4%; yield: 39%; white solid; mp: 119–121 °C;  $^1\text{H}$  NMR ( $\text{CDCl}_3$ ):  $\delta$  7.82 (brs, 4H, Ar), 6.31 (brs, 1H, Ar), 6.16–6.15 (m, 2H, Ar), 3.88 (t, 2H,  $J = 7.0$  Hz,  $\text{CH}_2$ ), 3.68 (s, 6H,  $\text{CH}_3$ ), 2.65 (t, 2H,  $J = 7.4$  Hz,  $\text{CH}_2$ ), 2.25–2.15 (m, 2H,  $\text{CH}_2$ );  $^{13}\text{C}$  NMR ( $\text{CDCl}_3$ ):  $\delta$  174.9, 161.0, 151.0, 144.5, 129.7, 129.5, 118.7, 100.8, 99.3, 55.5, 48.4, 32.8, 17.7; HRMS (ESI)  $m/z$  found, 378.0998;  $\text{C}_{18}\text{H}_{20}\text{NO}_6\text{S}$  ( $\text{M}^+ + \text{H}$ ) expected, 378.1012.

**5.2.6.12. 3,5-Dibromophenyl 4-(2-oxopyrrolidin-1-yl)benzenesulfonate (15).** Flash chromatography (hexanes/ethyl acetate (80:20) to (60:40)). Purity: 99.5%; yield: 54%; white solid; mp: 138–139 °C;  $^1\text{H}$  NMR ( $\text{CDCl}_3$ ):  $\delta$  7.86–7.75 (m, 4H, Ar), 7.51 (s, 1H, Ar), 7.11 (s, 2H, Ar), 3.87 (t, 2H,  $J = 7.0$  Hz,  $\text{CH}_2$ ), 2.63 (t, 2H,  $J = 8.0$  Hz,  $\text{CH}_2$ ), 2.24–2.16 (m, 2H,  $\text{CH}_2$ );  $^{13}\text{C}$  NMR ( $\text{CDCl}_3$ ):  $\delta$  175.1, 149.9, 145.0, 133.0, 129.5, 128.6, 124.6, 122.9, 118.9, 48.3, 32.8, 17.7; HRMS (ESI)  $m/z$  found,

473.9003;  $\text{C}_{16}\text{H}_{14}\text{Br}_2\text{NO}_4\text{S}$  ( $\text{M}^+ + \text{H}$ ) expected, 473.9009.

**5.2.6.13. 3,4,5-Trimethoxyphenyl 4-(2-oxopyrrolidin-1-yl)benzenesulfonate (16).** Flash chromatography (hexanes/ethyl acetate (80:20) to (60:40)). Purity: 96.5%; yield: 67%; pale solid; mp: 129–131 °C;  $^1\text{H}$  NMR ( $\text{CDCl}_3$ ):  $\delta$  7.77 (brs, 4H, Ar), 6.17 (s, 2H, Ar), 3.84 (t, 2H,  $J = 7.0$  Hz,  $\text{CH}_2$ ), 3.73 (s, 3H,  $\text{CH}_3$ ), 3.65 (s, 6H,  $\text{CH}_3$ ), 2.60 (t, 2H,  $J = 8.0$  Hz,  $\text{CH}_2$ ), 2.18–2.13 (m, 2H,  $\text{CH}_2$ );  $^{13}\text{C}$  NMR ( $\text{CDCl}_3$ ):  $\delta$  175.0, 153.3, 145.4, 144.5, 136.7, 129.6, 129.3, 118.8, 99.8, 60.9, 56.2, 48.3, 32.8, 17.7; HRMS (ESI)  $m/z$  found, 408.1115;  $\text{C}_{19}\text{H}_{22}\text{NO}_7\text{S}$  ( $\text{M}^+ + \text{H}$ ) expected, 408.1119.

**5.2.6.14. 4-Methoxyphenyl 4-(2-oxopyrrolidin-1-yl)benzenesulfonate (17).** Flash chromatography (methylene chloride/ethyl acetate (98:2)). Purity: 100.0%; yield: 42%; white solid; mp: 120–121 °C;  $^1\text{H}$  NMR ( $\text{CDCl}_3$ ):  $\delta$  7.83–7.74 (m, 4H, Ar), 6.88–6.85 (m, 2H, Ar), 6.76–6.73 (m, 2H, Ar), 3.89 (t, 2H,  $J = 7.0$  Hz,  $\text{CH}_2$ ), 3.75 (s, 3H,  $\text{CH}_3$ ), 2.65 (t, 2H,  $J = 8.0$  Hz,  $\text{CH}_2$ ), 2.25–2.15 (m, 2H,  $\text{CH}_2$ );  $^{13}\text{C}$  NMR ( $\text{CDCl}_3$ ):  $\delta$  175.0, 158.2, 144.4, 143.0, 129.6, 129.5, 123.3, 118.7, 114.5, 55.6, 48.4, 32.8, 17.7; HRMS (ESI)  $m/z$  found, 348.0898;  $\text{C}_{17}\text{H}_{18}\text{NO}_5\text{S}$  ( $\text{M}^+ + \text{H}$ ) expected, 348.0906.

**5.2.6.15. [1,1'-Biphenyl]-4-yl 4-(2-oxopyrrolidin-1-yl)benzenesulfonate (18).** Flash chromatography (methylene chloride/ethyl acetate (90:10)). Purity: 99.9%; yield: 36%; white solid; mp: 145–147 °C;  $^1\text{H}$  NMR ( $\text{CDCl}_3$ ):  $\delta$  7.85–7.79 (m, 4H, Ar), 7.52–7.31 (m, 7H, Ar), 7.05–7.02 (m, 2H, Ar), 3.88 (t, 2H,  $J = 7.0$  Hz,  $\text{CH}_2$ ), 2.65 (t, 2H,  $J = 8.0$  Hz,  $\text{CH}_2$ ), 2.24–2.17 (m, 2H,  $\text{CH}_2$ );  $^{13}\text{C}$  NMR ( $\text{CDCl}_3$ ):  $\delta$  175.0, 148.9, 144.6, 140.2, 139.7, 129.6, 129.5, 128.9, 128.3, 127.7, 127.1, 122.6, 118.8, 48.4, 32.9, 17.7; HRMS (ESI)  $m/z$  found, 394.1103;  $\text{C}_{22}\text{H}_{20}\text{NO}_4\text{S}$  ( $\text{M}^+ + \text{H}$ ) expected, 394.1109.

### 5.2.7. General preparation of compounds 19–33

The relevant aniline (1.5 Eq) was added to a solution of the 4-(2-oxopyrrolidin-1-yl)benzenesulfonyl chloride (**36**, 0.10 g) in acetonitrile (3.0 mL) in presence of 4-dimethylaminopyridine (0.14 g, 3.0 Eq). The reaction mixture was stirred at 120 °C under microwave radiations for 8 h. The mixture was cooled at room temperature and the solvent was evaporated under reduced pressure. The residue was diluted with AcOEt (10 mL) and washed twice with HCl 1M (10 mL) and brine (10 mL). The resulting solution was dried over anhydrous sodium sulfate, filtered and evaporated to dryness under reduced pressure. The residue was purified by flash chromatography on silica gel.

### 5.2.8. Characterization of compounds 19–33

**5.2.8.1. 4-(2-Oxopyrrolidin-1-yl)-N-phenylbenzenesulfonamide (19).** Flash chromatography (methylene chloride to methylene chloride/ethyl acetate (90:10)). Purity: 100.0%; yield: 38%; white solid; mp: 184–186 °C;  $^1\text{H}$  NMR ( $\text{DMSO}-d_6$ ):  $\delta$  10.20 (s, 1H, NH), 7.81–7.70 (m, 4H, Ar), 7.22–7.17 (m, 2H, Ar), 7.08–6.96 (m, 3H, Ar), 3.79 (t, 2H,  $J = 6.9$  Hz,  $\text{CH}_2$ ), 2.48 (t, 2H,  $J = 7.8$  Hz,  $\text{CH}_2$ ), 2.06–1.96 (m, 2H,  $\text{CH}_2$ );  $^{13}\text{C}$  NMR ( $\text{DMSO}-d_6$ ):  $\delta$  175.2, 143.5, 138.2, 134.0, 129.6, 128.1, 124.4, 120.4, 119.1, 48.3, 32.9, 17.7; HRMS (ESI)  $m/z$  found, 317.0957;  $\text{C}_{16}\text{H}_{17}\text{N}_2\text{O}_3\text{S}$  ( $\text{M}^+ + \text{H}$ ) expected, 317.0961.

**5.2.8.2. N-(2-Isopropylphenyl)-4-(2-oxopyrrolidin-1-yl)benzenesulfonamide (20).** Flash chromatography (methylene chloride/ethyl acetate (95:5)). Purity: 96.8%; yield: 39%; white solid; mp: 179–181 °C;  $^1\text{H}$  NMR ( $\text{DMSO}-d_6$ ):  $\delta$  9.60 (s, 1H, NH), 7.89–7.86 (m, 2H, Ar), 7.71–7.69 (m, 2H, Ar), 7.31–7.18 (m, 2H, Ar), 7.09–7.05 (m, 1H, Ar), 6.90–6.87 (m, 1H, Ar), 3.86 (t, 2H,  $J = 6.9$  Hz,  $\text{CH}_2$ ), 3.30–3.25 (m, 1H, CH), 2.56 (t, 2H,  $J = 8.0$  Hz,  $\text{CH}_2$ ), 2.11–2.06 (m, 2H,  $\text{CH}_2$ ), 1.00 (d, 6H,  $J = 6.7$  Hz,  $\text{CH}_3$ );  $^{13}\text{C}$  NMR ( $\text{DMSO}-d_6$ ):  $\delta$  175.1, 146.3, 143.4, 135.3, 133.6, 128.1, 127.8, 127.7, 126.8, 126.3, 119.1, 48.5,

32.9, 27.2, 24.0, 17.7; HRMS (ESI)  $m/z$  found, 359.1423;  $C_{19}H_{23}N_2O_3S$  ( $M^+ + H$ ) expected, 359.1429.

5.2.8.3. *N-([1,1'-Biphenyl]-2-yl)-4-(2-oxopyrrolidin-1-yl)benzenesulfonamide (21)*. Flash chromatography (methylene chloride to methylene chloride/ethyl acetate (95:5)). Purity: 98.0%; yield: 52%; pale yellow solid; mp: 104–106 °C;  $^1H$  NMR (DMSO- $d_6$ ):  $\delta$  9.42 (s, 1H, NH), 7.77–7.74 (m, 2H, Ar), 7.57–7.54 (m, 2H, Ar), 7.34–7.21 (m, 8H, Ar), 7.08–7.05 (m, 1H, Ar), 3.83 (t, 2H,  $J = 6.9$  Hz, CH<sub>2</sub>), 2.55–2.50 (m, 2H, CH<sub>2</sub>), 2.10–2.02 (m, 2H, CH<sub>2</sub>);  $^{13}C$  NMR (DMSO- $d_6$ ):  $\delta$  175.1, 143.3, 139.0, 139.0, 135.5, 133.8, 131.4, 129.7, 128.5, 128.4, 127.8, 127.5, 127.1, 126.9, 119.1, 48.4, 32.9, 17.7; HRMS (ESI)  $m/z$  found, 393.1266;  $C_{22}H_{21}N_2O_3S$  ( $M^+ + H$ ) expected, 393.1269.

5.2.8.4. *N-(2-Methoxyphenyl)-4-(2-oxopyrrolidin-1-yl)benzenesulfonamide (22)*. Flash chromatography (methylene chloride to methylene chloride/ethyl acetate (95:5)). Purity: 100.0%; yield: 39%; pale solid; mp: 190–192 °C;  $^1H$  NMR (CDCl<sub>3</sub>):  $\delta$  7.74–7.65 (m, 4H, Ar), 7.51–7.49 (m, 1H, Ar), 7.05–6.98 (m, 2H, Ar and NH), 6.89–6.84 (m, 1H, Ar), 6.73–6.70 (m, 1H, Ar), 3.81 (t, 2H,  $J = 7.0$  Hz, CH<sub>2</sub>), 3.64 (s, 3H, CH<sub>3</sub>), 2.60 (t, 2H,  $J = 8.0$  Hz, CH<sub>2</sub>), 2.19–2.09 (m, 2H, CH<sub>2</sub>);  $^{13}C$  NMR (CDCl<sub>3</sub>):  $\delta$  174.8, 149.4, 143.3, 133.8, 128.2, 125.8, 125.3, 121.1, 120.9, 118.7, 110.6, 55.7, 48.4, 32.8, 17.7; HRMS (ESI)  $m/z$  found, 347.1058;  $C_{17}H_{18}N_2O_4S$  ( $M^+ + H$ ) expected, 347.1066.

5.2.8.5. *N-(3-Methoxyphenyl)-4-(2-oxopyrrolidin-1-yl)benzenesulfonamide (23)*. Flash chromatography (methylene chloride/ethyl acetate (95:5)). Purity: 99.8%; yield: 62%; brown solid; mp: 173–175 °C;  $^1H$  NMR (DMSO- $d_6$ ):  $\delta$  10.24 (s, 1H, NH), 7.82–7.73 (m, 4H, Ar), 7.12–7.06 (m, 1H, Ar), 6.67–6.54 (m, 3H, Ar), 3.77 (t, 2H,  $J = 6.9$  Hz, CH<sub>2</sub>), 3.63 (s, 3H, CH<sub>3</sub>), 2.47 (t, 2H,  $J = 7.8$  Hz, CH<sub>2</sub>), 2.02–1.97 (m, 2H, CH<sub>2</sub>);  $^{13}C$  NMR (DMSO- $d_6$ ):  $\delta$  175.2, 160.1, 143.6, 139.5, 134.0, 130.4, 128.1, 119.1, 112.2, 109.3, 106.0, 55.4, 48.3, 32.8, 17.7; HRMS (ESI)  $m/z$  found, 347.1057;  $C_{17}H_{19}N_2O_4S$  ( $M^+ + H$ ) expected, 347.1066.

5.2.8.6. *N-(3-Fluorophenyl)-4-(2-oxopyrrolidin-1-yl)benzenesulfonamide (24)*. Flash chromatography (hexanes/ethyl acetate (63:37)). Purity: 99.6%; yield: 39%; white solid; mp: 206–208 °C;  $^1H$  NMR (DMSO- $d_6$ ):  $\delta$  10.53 (s, 1H, NH), 7.84–7.75 (m, 4H, Ar), 7.27–7.20 (m, 1H, Ar), 6.91–6.78 (m, 3H, Ar), 3.79 (t, 2H,  $J = 6.9$  Hz, CH<sub>2</sub>), 2.48 (t, 2H,  $J = 7.9$  Hz, CH<sub>2</sub>), 2.05–1.95 (m, 2H, CH<sub>2</sub>);  $^{13}C$  NMR (DMSO- $d_6$ ):  $\delta$  175.2, 164.3, 161.1, 143.8, 140.2, 140.1, 133.6, 131.5, 131.3, 128.1, 119.2, 115.7, 115.6, 110.9, 110.7, 106.7, 106.4, 48.3, 32.9, 17.7; HRMS (ESI)  $m/z$  found, 335.0859;  $C_{16}H_{16}FN_2O_3S$  ( $M^+ + H$ ) expected, 335.0866.

5.2.8.7. *N-(3-Chlorophenyl)-4-(2-oxopyrrolidin-1-yl)benzenesulfonamide (25)*. Flash chromatography (methylene chloride/ethyl acetate (95:5)). Purity: 99.7%; yield: 43%; white solid; mp: 187–189 °C;  $^1H$  NMR (DMSO- $d_6$ ):  $\delta$  10.52 (s, 1H, NH), 7.84–7.74 (m, 4H, Ar), 7.26–7.20 (m, 1H, Ar), 7.10–7.03 (m, 3H, Ar), 3.81 (t, 2H,  $J = 6.9$  Hz, CH<sub>2</sub>), 2.48 (t, 2H,  $J = 7.9$  Hz, CH<sub>2</sub>), 2.06–1.98 (m, 2H, CH<sub>2</sub>);  $^{13}C$  NMR (DMSO- $d_6$ ):  $\delta$  175.2, 143.8, 139.9, 133.8, 133.5, 131.4, 128.1, 124.1, 119.3, 119.2, 118.3, 48.3, 32.9, 17.7; HRMS (ESI)  $m/z$  found, 351.0561;  $C_{16}H_{16}ClN_2O_3S$  ( $M^+ + H$ ) expected, 351.0571.

5.2.8.8. *N-(3-Bromophenyl)-4-(2-oxopyrrolidin-1-yl)benzenesulfonamide (26)*. Flash chromatography (methylene chloride/ethyl acetate (95:5)). Purity: 100.0%; yield: 56%; pale solid; mp: 195–198 °C;  $^1H$  NMR (DMSO- $d_6$ ):  $\delta$  10.50 (s, 1H, NH), 7.84–7.74 (m, 4H, Ar), 7.24–7.09 (m, 4H, Ar), 3.79 (t, 2H,  $J = 6.9$  Hz, CH<sub>2</sub>), 2.48 (t, 2H,  $J = 7.9$  Hz, CH<sub>2</sub>), 2.06–1.98 (m, 2H, CH<sub>2</sub>);  $^{13}C$  NMR (DMSO- $d_6$ ):  $\delta$  175.2, 143.8, 140.0, 133.5, 131.7, 128.1, 127.0, 122.2, 122.2, 119.2,

118.6, 48.3, 32.9, 17.7; HRMS (ESI)  $m/z$  found, 395.0049;  $C_{16}H_{16}BrN_2O_3S$  ( $M^+ + H$ ) expected, 395.0066.

5.2.8.9. *N-(3-Iodophenyl)-4-(2-oxopyrrolidin-1-yl)benzenesulfonamide (27)*. Flash chromatography (methylene chloride/ethyl acetate (95:5)). Purity: 99.4%; yield: 54%; pale solid; mp: 188–190 °C;  $^1H$  NMR (DMSO- $d_6$ ):  $\delta$  10.41 (s, 1H, NH), 7.84–7.73 (m, 4H, Ar), 7.42–7.32 (m, 2H, Ar), 7.13–6.97 (m, 2H, Ar), 3.79 (t, 2H,  $J = 6.9$  Hz, CH<sub>2</sub>), 2.48 (t, 2H,  $J = 7.9$  Hz, CH<sub>2</sub>), 2.05–1.96 (m, 2H, CH<sub>2</sub>);  $^{13}C$  NMR (DMSO- $d_6$ ):  $\delta$  175.2, 143.8, 139.7, 133.6, 132.9, 131.6, 128.1, 128.1, 119.2, 119.0, 95.3, 48.3, 32.9, 17.7; HRMS (ESI)  $m/z$  found, 442.9908;  $C_{16}H_{16}IN_2O_3S$  ( $M^+ + H$ ) expected, 442.9927.

5.2.8.10. *N-(3,4-Dimethoxyphenyl)-4-(2-oxopyrrolidin-1-yl)benzenesulfonamide (28)*. Flash chromatography (methylene chloride/ethyl acetate (95:5)). Purity: 97.2%; yield: 67%; pale solid; mp: 184–187 °C;  $^1H$  NMR (DMSO- $d_6$ ):  $\delta$  9.84 (s, 1H, NH), 7.80–7.77 (m, 2H, Ar), 7.69–7.66 (m, 2H, Ar), 6.77–6.69 (m, 2H, Ar), 6.54–6.51 (m, 1H, Ar), 3.79 (t, 2H,  $J = 6.8$  Hz, CH<sub>2</sub>), 3.63–3.62 (m, 6H, CH<sub>3</sub>), 2.49 (t, 2H,  $J = 8.0$  Hz, CH<sub>2</sub>), 2.06–1.97 (m, 2H, CH<sub>2</sub>);  $^{13}C$  NMR (DMSO- $d_6$ ):  $\delta$  175.1, 149.2, 146.4, 143.4, 134.0, 131.1, 128.1, 119.0, 112.4, 106.7, 56.0, 55.8, 48.3, 32.9, 17.7; HRMS (ESI)  $m/z$  found, 377.1158;  $C_{18}H_{21}N_2O_5S$  ( $M^+ + H$ ) expected, 377.1172.

5.2.8.11. *N-(3,5-Dimethoxyphenyl)-4-(2-oxopyrrolidin-1-yl)benzenesulfonamide (29)*. Flash chromatography (methylene chloride/ethyl acetate (95:5)). Purity: 96.6%; yield: 60%; white solid; mp: 177–179 °C;  $^1H$  NMR (DMSO- $d_6$ ):  $\delta$  10.23 (s, 1H, NH), 7.82–7.75 (m, 4H, Ar), 6.28–6.13 (m, 3H, Ar), 3.76 (t, 2H,  $J = 6.8$  Hz, CH<sub>2</sub>), 3.62 (s, 6H, CH<sub>3</sub>), 2.47 (t, 2H,  $J = 7.8$  Hz, CH<sub>2</sub>), 2.02–1.97 (m, 2H, CH<sub>2</sub>);  $^{13}C$  NMR (DMSO- $d_6$ ):  $\delta$  175.2, 161.2, 143.6, 140.1, 133.9, 128.2, 119.1, 98.1, 95.5, 55.5, 48.3, 32.8, 17.7; HRMS (ESI)  $m/z$  found, 377.1154;  $C_{18}H_{21}N_2O_5S$  ( $M^+ + H$ ) expected, 377.1172.

5.2.8.12. *N-(3,5-Dibromophenyl)-4-(2-oxoimidazolidin-1-yl)benzenesulfonamide (30)*. Flash chromatography (methylene chloride/ethyl acetate (95:5)). Purity: 96.9%; yield: 18%; white solid; mp: 244–246 °C;  $^1H$  NMR (DMSO- $d_6$ ):  $\delta$  10.77 (s, 1H, NH), 7.88–7.85 (m, 2H, Ar), 7.79–7.76 (m, 2H, Ar), 7.44 (s, 1H, Ar), 7.25 (s, 2H, Ar), 3.82 (t, 2H,  $J = 6.9$  Hz, CH<sub>2</sub>), 2.50–2.48 (m, 2H, CH<sub>2</sub>), 2.07–1.98 (m, 2H, CH<sub>2</sub>);  $^{13}C$  NMR (DMSO- $d_6$ ):  $\delta$  175.3, 144.0, 141.2, 133.1, 128.8, 128.1, 123.2, 120.8, 119.3, 48.3, 32.9, 17.7; HRMS (ESI)  $m/z$  found, 472.9156;  $C_{16}H_{15}Br_2N_2O_3S$  ( $M^+ + H$ ) expected, 472.9169.

5.2.8.13. *4-(2-Oxopyrrolidin-1-yl)-N-(3,4,5-trimethoxyphenyl)benzenesulfonamide (31)*. Flash chromatography (methylene chloride/ethyl acetate (95:5)). Purity: 97.1%; yield: 47%; pale solid; mp: 199–201 °C;  $^1H$  NMR (DMSO- $d_6$ ):  $\delta$  10.07 (s, 1H, NH), 7.83–7.75 (m, 4H, Ar), 6.39 (s, 2H, Ar), 3.78 (t, 2H,  $J = 6.7$  Hz, CH<sub>2</sub>), 3.64 (s, 6H, CH<sub>3</sub>), 3.53 (s, 3H, CH<sub>3</sub>), 2.48 (t, 2H,  $J = 7.8$  Hz, CH<sub>2</sub>), 2.03–1.98 (m, 2H, CH<sub>2</sub>);  $^{13}C$  NMR (DMSO- $d_6$ ):  $\delta$  175.2, 153.4, 143.6, 134.4, 134.2, 133.9, 128.3, 119.1, 98.0, 60.5, 56.2, 48.3, 32.8, 17.7; HRMS (ESI)  $m/z$  found, 407.1269;  $C_{19}H_{23}N_2O_6S$  ( $M^+ + H$ ) expected, 407.1278.

5.2.8.14. *N-(4-Methoxyphenyl)-4-(2-oxopyrrolidin-1-yl)benzenesulfonamide (32)*. Flash chromatography (methylene chloride/ethyl acetate (95:5)). Purity: 97.1%; yield: 18%; pale brown solid; mp: 206–209 °C;  $^1H$  NMR (DMSO- $d_6$ ):  $\delta$  9.83 (s, 1H, NH), 7.80–7.62 (m, 4H, Ar), 6.97–6.76 (m, 4H, Ar), 3.80 (t, 2H,  $J = 6.9$  Hz, CH<sub>2</sub>), 3.64 (s, 3H, CH<sub>3</sub>), 2.52–2.47 (m, 2H, CH<sub>2</sub>), 2.07–2.00 (m, 2H, CH<sub>2</sub>);  $^{13}C$  NMR (DMSO- $d_6$ ):  $\delta$  175.2, 156.9, 143.4, 134.0, 130.7, 128.1, 123.8, 119.0, 114.7, 55.6, 48.4, 32.9, 17.7; HRMS (ESI)  $m/z$  found, 347.1061;  $C_{17}H_{19}N_2O_4S$  ( $M^+ + H$ ) expected, 347.1066.

5.2.8.15. *N*-([1,1'-biphenyl]-4-yl)-4-(2-oxopyrrolidin-1-yl)benzenesulfonamide (**33**). Flash chromatography (methylene chloride/ethyl acetate (95:5) to (85:15)). Purity: 98.2%; yield: 54%; white solid; mp: 177–179 °C; <sup>1</sup>H NMR (DMSO-*d*<sub>6</sub>): δ 10.35, (s, 1H, NH), 7.83–7.76 (m, 4H, Ar), 7.56–7.51 (m, 4H, Ar), 7.41–7.26 (m, 3H, Ar), 7.19–7.16 (m, 2H, Ar), 3.78 (t, 2H, *J* = 6.9 Hz, CH<sub>2</sub>), 2.50–2.47 (m, 2H, CH<sub>2</sub>), 2.05–1.95 (m, 2H, CH<sub>2</sub>); <sup>13</sup>C NMR (DMSO-*d*<sub>6</sub>): δ 175.2, 143.6, 139.7, 137.7, 136.0, 134.1, 129.3, 128.1, 127.8, 127.6, 126.7, 120.5, 119.2, 48.3, 32.9, 17.7; HRMS (ESI) *m/z* found, 393.1256; C<sub>22</sub>H<sub>21</sub>N<sub>2</sub>O<sub>3</sub>S (M<sup>+</sup> + H) expected, 393.1269.

### 5.3. In silico methods

#### 5.3.1. Docking studies

Molecular modelling calculations and docking studies were performed using Molecular Operating Environment (MOE) version 2019.01". PYB-SOs **14** and **15**, PYB-SAs **30** and **31** and CA-4 were drawn with ChemBioDraw 13.0 software and imported to MOE as SDF file for docking experiments. The X-ray crystallographic structure of the α, β-tubulin heterodimer was obtained from the RCSB protein data bank (PDB: 1SA0) and loaded to MOE software. The protein was prepared using the QuickPrep tool with default settings to add hydrogens and partial charges, correct Asn/Gln/His orientations, optimise the H-bond network (protonate 3D), delete water molecules farther than 4.5 Å from the ligand and the receptor, and perform an energy minimisation (RMS gradient of 0.1 kcal/mol/Å). Then, a second energy minimisation was performed prior to the docking of α, β-tubulin heterodimer inhibitors. The default settings were applied to all atoms and included the absence of restriction, a force field Amber10 (ETH; R-Field 1:80; Cutoff [8,10]), system appearing reasonable for the charges, the rigidity of the water molecules and a gradient of 0.1 RMS kcal/mol/Å<sup>2</sup>. The surface hydrophobicity (green) and hydrophilicity (brown) of the C-BS was mapped using the Surface and Map Surface and Map tool with default settings. The ligand was isolated and the binding site was created with the amino acids in the vicinity of colchicine and GTP. The binding site was constituted of GTP and 32 amino acids: Gln11, Asn101, Ser178, Thr179, Ala180, Val181, Val215, Tyr224, Val238, Cys241, Leu242, Gln247, Leu248, Asn249, Ala250, Asp251, Lys254, Leu255, Asn258, Met259, Thr314, Val315, Ala316, Ala317, Val318, Asn349, Asn350, Val351, Lys352, Thr353, Ala354 and Ile378. Selected PYB-SOs and PYB-SAs were docked into the C-BS using the selected atoms from the receptor and the selected residues from the binding site. The different conformations, the interactions with the amino acids of the active site and the energies of the complexes were analysed and recorded. Pictures of the most stable conformers in the C-BS site were taken in 3D and 2D models.

### Declaration of competing interest

The authors declare that they have no known competing financial interests or personal relationships that could have appeared to influence the work reported in this paper.

### Acknowledgments

This work was supported by grants from Natural Sciences and Engineering Research Council of Canada (NSERC, RGPIN-2016-05069), Fonds de Recherche du Québec – Santé (starting grant for new investigators) and CHU de Québec–Université Laval Research Center. S. Fortin holds a Junior 1 research scholar award from Fonds de Recherche du Québec – Santé (FRQS). M. Gagné-Boulet and C. Bouzriba are recipients of studentships from the Fonds d'enseignement et de recherche of the Faculty of pharmacy of Université Laval and Fonds de recherche du Québec-Santé (FRQS),

respectively. A.C. Chavez Alvarez is recipient of studentships from Fonds d'enseignement et de recherche of the Faculty of pharmacy of Université Laval.

### Appendix B. Supplementary data

Supplementary data to this article can be found online at <https://doi.org/10.1016/j.ejmech.2020.113136>.

### References

- [1] R.L. Siegel, K.D. Miller, A. Jemal, Cancer statistics, *CA Cancer J Clin* 69 (2019) 7–34, 2019.
- [2] Cancer World Health Organization. <https://www.who.int/en/news-room/fact-sheets/detail/cancer> accessed december 20<sup>th</sup>, 2019.
- [3] E. Mazzotti, G.C.A. Cappellini, S. Buconovo, R. Morese, A. Scoppola, C. Sebastiani, P. Marchetti, Treatment-related side effects and quality of life in cancer patients, *Support. Care Cancer* 20 (2012) 2553–2557.
- [4] J. Ferlay, M. Colombet, I. Soerjomataram, C. Mathers, D.M. Parkin, M. Pineros, A. Znaor, F. Bray, Estimating the global cancer incidence and mortality in 2018: GLOBOCAN sources and methods, *Int. J. Canc.* 144 (2019) 1941–1953.
- [5] J. Lowe, H. Li, K.H. Downing, E. Nogales, Refined structure of αβ-tubulin at 3.5 Å resolution, *J. Mol. Biol.* 313 (2001) 1045–1057.
- [6] D.A. Fletcher, R.D. Mullins, Cell mechanics and the cytoskeleton, *Nature* 463 (2010) 485–492.
- [7] E.K. Rowinsky, R.C. Donehower, Paclitaxel (taxol), *N. Engl. J. Med.* 332 (1995) 1004–1014.
- [8] M.A. Jordan, L. Wilson, Microtubules as a target for anticancer drugs, *Nat. Rev. Canc.* 4 (2004) 253–265.
- [9] S.R. Nasrin, A.M. Rashedul Kabir, A. Konagaya, T. Ishihara, K. Sada, A. Kakugo, Stabilization of microtubules by cevipabulin, *Biochem. bioph. res. Co.* 516 (2019) 760–764.
- [10] A study of E7130 in participants with solid tumors. <https://clinicaltrials.gov/ct2/show/NCT03444701> accessed November 23<sup>th</sup>, 2020.
- [11] A.M. Olzierys, S.I. Labidi-Galy, Clinical development of anti-mitotic drugs in cancer, *Adv. Exp. Med. Biol.* 1002 (2017) 125–152.
- [12] G.C. Tron, T. Pirali, G. Sorba, F. Pagliai, S. Busacca, A.A. Genazzani, Medicinal chemistry of combretastatin A4: Present and future directions, *J. Med. Chem.* 49 (2006) 3033–3044.
- [13] B. Shan, J.C. Medina, E. Santha, W.P. Frankmoelle, T.C. Chou, R.M. Learned, M.R. Narbut, D. Stott, P.G. Wu, J.C. Jaen, T. Rosen, P. Timmermans, H. Beckmann, Selective, covalent modification of β-tubulin residue Cys-239 by T138067, an antitumor agent with *in vivo* efficacy against multidrug-resistant tumors, *Proc. Natl. Acad. Sci. U. S. A.* 96 (1999) 5686–5691.
- [14] S. Fortin, L.H. Wei, E. Moreau, J. Lacroix, M.-F. Côté, É. Petitclerc, L.P. Kotra, R.C. Gaudreault, Design, synthesis, biological evaluation, and structure-activity relationships of substituted phenyl 4-(2-oxoimidazolidin-1-yl)benzenesulfonates as new tubulin inhibitors mimicking combretastatin A-4, *J. Med. Chem.* 54 (2011) 4559–4580.
- [15] S. Fortin, L. Wei, E. Moreau, J. Lacroix, M.-F. Côté, É. Petitclerc, L.P. Kotra, R.C. Gaudreault, Substituted phenyl 4-(2-oxoimidazolidin-1-yl)benzenesulfonamides as antimicrotubule agents. Antiproliferative, antiangiogenic and antitumor activity, and quantitative structure-activity relationships, *Eur. J. Med. Chem.* 46 (2011) 5327–5342.
- [16] S. Fortin, L. Wei, L.P. Kotra, R.C. Gaudreault, Novel cytoskeletal substituted phenyl 4-(2-oxoimidazolidin-1-yl) benzenesulfonates and benzenesulfonamides with affinity to the colchicine-binding site: is the phenyl 2-imidazolidinone moiety a new haptophore for the design of new antimicrotubule agents? *Open J. Med. Chem.* 5 (2015) 14.
- [17] M. Zarifi Khosroshahi, A.C. Chavez Alvarez, M. Gagné-Boulet, R.C. Gaudreault, S. Gobeil, S. Fortin, Evaluation of the time-dependent antiproliferative activity and liver microsome stability of 3 phenyl 4-(2-oxo-3-alkylimidazolidin-1-yl) benzenesulfonates as promising CYP1A1-dependent antimicrotubule prodrugs 72 (2020) 249–258.
- [18] A. Daina, O. Michielin, V. Zoete, SwissADME: a free web tool to evaluate pharmacokinetics, drug-likeness and medicinal chemistry friendliness of small molecules, *Sci. Rep.* 7 (2017) 42717.
- [19] Tubulin polymerization assay using >99% pure tubulin, fluorescence based. <https://www.cytoskeleton.com/kits/tubulin-assays/bk011p> (accessed April 15<sup>th</sup>, 2020).
- [20] A.L. Risinger, F.J. Giles, S.L. Mooberry, Microtubule dynamics as a target in oncology, *Canc. Treat Rev.* 35 (2009) 255–261.
- [21] S. Fortin, J. Lacroix, M.-F. Côté, E. Moreau, É. Petitclerc, R.C. Gaudreault, Quick and simple detection technique to assess the binding of antimicrotubule agents to the colchicine-binding site, *Biol. Proced. Online* 12 (2010) 113–117.
- [22] R.B. Ravelli, B. Gigant, P.A. Curmi, I. Jourdain, S. Lachkar, A. Sobel, M. Knossow, Insight into tubulin regulation from a complex with colchicine and a stathmin-like domain, *Nature* 428 (2004) 198–202.
- [23] National Cancer Institute, NCI 60 cell five-dose screen. [https://dtp.cancer.gov/discovery\\_development/nci-60/default.htm](https://dtp.cancer.gov/discovery_development/nci-60/default.htm) (accessed April 29<sup>th</sup>, 2019).
- [24] Tubulin polymerization assay kit manual. <https://www.cytoskeleton.com/pdf->

- storage/datasheets/bk011p.pdf (accessed June 16<sup>th</sup>, 2020).
- [25] U.K. Laemmli, Cleavage of structural proteins during the assembly of the head of bacteriophage T4, *Nature* 227 (1970) 680–685.
- [26] E. Massolo, M. Pirola, A. Puglisi, S. Rossi, M. Benaglia, A one pot protocol to convert nitro-arenes into *N*-aryl amides, *RSC Adv.* 10 (2020) 4040–4044.
- [27] U. Ladziata, A.Y. Kuposov, K.Y. Lo, J. Willging, V.N. Nemykin, V.V. Zhdankin, Synthesis, structure, and chemoselective reactivity of *N*-(2-iodylphenyl)acylamides: hypervalent iodine reagents bearing a pseudo-six-membered ring scaffold, *Angew. Chem. Int. Ed.* 44 (2005) 7127–7131.
- [28] Y.-H. Yang, M. Shi, Ring-expanding reaction of cyclopropyl amides with triphenylphosphine and carbon tetrahalide, *J. Org. Chem.* 70 (2005) 8645–8648.
- [29] S.-Y. Lin, T.-K. Yeh, C.-C. Kuo, J.-S. Song, M.-F. Cheng, F.-Y. Liao, M.-W. Chao, H.-L. Huang, Y.-L. Chen, C.-Y. Yang, M.-H. Wu, C.-L. Hsieh, W. Hsiao, Y.-H. Peng, J.-S. Wu, L.-M. Lin, M. Sun, Y.-S. Chao, C. Shih, S.-Y. Wu, S.-L. Pan, M.-S. Hung, S.-H. Ueng, Phenyl benzenesulfonylhydrazides exhibit selective indoleamine 2,3-dioxygenase inhibition with potent *in vivo* pharmacodynamic activity and antitumor efficacy, *J. Med. Chem.* 59 (2016) 419–430.